

THESIS

ASSESSMENT, DESIGN AND CONTROL STRATEGY DEVELOPMENT OF A FUEL
CELL HYBRID ELECTRIC VEHICLE FOR CSU'S ECOCAR

Submitted by

Matthew D. Fox

Department of Mechanical Engineering

In partial fulfillment of the requirements

For the Degree of Master of Science

Colorado State University

Fort Collins, Colorado

Spring 2013

Master's Committee:

Advisor: Thomas H. Bradley

Dan Zimmerle

John Labadie

ABSTRACT

ASSESSMENT, DESIGN AND CONTROL STRATEGY DEVELOPMENT OF A FUEL CELL HYBRID ELECTRIC VEHICLE FOR CSU'S ECOCAR

Advanced automotive technology assessment and powertrain design are increasingly performed through modeling, simulation, and optimization. But technology assessments usually target many competing criteria making any individual optimization challenging and arbitrary. Further, independent design simulations and optimizations take considerable time to execute, and design constraints and objectives change throughout the design process. Changes in design considerations usually require re-processing of simulations and more time. In this thesis, these challenges are confronted through CSU's participation in the EcoCAR2 hybrid vehicle design competition. The complexity of the competition's design objectives leveraged development of a decision support system tool to aid in multi-criteria decision making across technologies and to perform powertrain optimization. To make the decision support system interactive, and bypass the problem of long simulation times, a new approach was taken. The result of this research is CSU's architecture selection and component sizing, which optimizes a composite objective function representing the competition score. The selected architecture is an electric vehicle with an onboard range extending hydrogen fuel cell system. The vehicle has a 145kW traction motor, 18.9kWh of lithium ion battery, a 15kW fuel cell system, and 5kg of hydrogen storage capacity. Finally, a control strategy was developed that improves the vehicles performance throughout the driving range under variable driving conditions

In conclusion, the design process used in this research is reviewed and evaluated against other common design methodologies. I conclude, through the highlighted case studies, that the approach is more comprehensive than other popular design methodologies and is likely to lead to a higher quality product. The hypothesis is supported by the three case studies examined in this thesis.

TABLE OF CONTENTS

1.0	Introduction.....	1
2.0	Vehicle Modeling.....	2
2.1	Models.....	2
2.2	Model Validation	6
2.2.1	Electric Vehicle	6
2.2.2	Parallel Hybrid Electric Vehicle.....	9
2.2.3	Fuel Cell Hybrid Electric Vehicle	11
2.3	Conclusion	13
3.0	Plug-in Fuel Cell Vehicle Technology and Value Analysis	14
3.1	Abstract.....	14
3.2	Introduction.....	15
3.3	Background.....	16
3.4	Methods.....	18
3.4.1	Drive Cycles	19
3.4.2	Design Variables.....	19
3.4.3	Design Metrics.....	20
3.5	Results.....	22
3.5.1	Vehicle Benchmarking	22
3.5.2	Increased Breadth of Design Space	23
3.5.3	Increased Vehicle Design Detail	25
3.6	Discussion	28
3.7	Conclusions.....	30
4.0	Technology Assessment and High-Level Design Optimization for EcoCAR2	31
4.1	Abstract.....	31
4.2	Introduction.....	32
4.3	Methods.....	33
4.3.1	Design Metrics.....	34
4.3.2	Decision Support System.....	39
4.4	Results.....	42
5.0	Detailed Design and Control Strategy Development of a Plug-in Fuel Cell Hybrid Electric Vehicle for CSU's EcoCAR.....	49
5.1	Introduction.....	49
5.2	Methods.....	51
5.3	Results.....	52
5.3.1	EV Range vs Competition Score	52
5.3.2	Supervisory Control Strategy Development.....	54
5.4	Discussion.....	58
6.0	Conclusions.....	59
7.0	References.....	60

TABLE OF FIGURES

Figure 1 Efficiency maps and ideal operating lines for E10 (left), E85 (middle), and B20 (right) engines 4

Figure 2 Efficiency maps for electric motor/generator (left), Li-ion battery (mid), and fuel cell system (right) 4

Figure 3 BEV energy loss validation on US06 cycle vs Autonomie 7

Figure 4 BEV simulation validation on US06 cycle vs Autonomie 8

Figure 5 Parallel HEV energy loss validation on US06 cycle vs Autonomie 9

Figure 6 Parallel HEV simulation validation on US06 cycle vs Autonomie..... 10

Figure 7 Fuel Cell HEV energy loss validation on US06 cycle vs Autonomie 11

Figure 8 Fuel Cell HEV simulation validation on US06 cycle vs Autonomie 12

Figure 9 U.S. and California electricity mix WTW GHG emissions comparison for seven representative vehicles from Phase 1 study. 17

Figure 10 Near- and long-term fuel costs comparison for seven representative vehicles from Phase 1 study..... 17

Figure 11 Benchmarking of simulations against commercially available vehicles 23

Figure 12 Vehicle design space power-to-weight ratio vs. utility factor. 23

Figure 13 Vehicle designs near term fuel costs vs. U.S. electricity mix WTW GHGs, “worst case” scenario..... 24

Figure 14 Vehicle designs long-term fuel costs vs. CA electricity mix WTW GHGs, “best case” scenario. 24

Figure 15 Pareto-optimal vehicles for U.S. and CA GHG emissions, by degree of hybridization. 26

Figure 16 Pareto-optimal vehicles for U.S. and CA GHG emissions, by total vehicle power. 26

Figure 17 Pareto-optimal vehicles for U.S. and CA GHG emissions, by battery energy storage capacity. 26

Figure 18 Pareto-optimal vehicles for near term and long term fuel costs, by degree of hybridization. 27

Figure 19 Pareto-optimal vehicles for near term and long term fuel costs, by total vehicle power. 27

Figure 20 Pareto-optimal vehicles for near term and long term fuel costs, by battery energy storage capacity..... 28

Figure 21 Decision support system data flow 34

Figure 22 Decision support system user interface 42

Figure 23 Pareto-optimal E&EC Score over CD range (subject to: 0-60mph<8sec and gradeability>3.5%) 44

Figure 24 Series H2 PFCV Pareto-optimal inverse design space (optimized design point shown in red) 46

Figure 25 Selected Architecture, Fuel, and Components based on the results of this study 48

Figure 26 Passive fuel cell system efficiency (left), automotive fuel cell system efficiency (right) 50

Figure 27 Electric only to blended-charge-depleting control strategy representation 51

Figure 28 EV Range vs FC power and operating point 53

Figure 29 EcoCAR2 Score vs Fuel Cell size and operating point 53

Figure 30 Pareto tradeoff between EcoCAR score and fuel cell system power using the optimal blended charge depleting control strategy 54

Figure 31 Supervisory control strategy diagram.....	55
Figure 32 State of charge of battery and hydrogen tank under the blended charge depleting control strategy.....	55
Figure 33 State of charge of battery and tank (with tank starting at 50%)	56
Figure 34 Control strategy in variable driving conditions (NREL to Vail, CO and back)	57
Figure 35 Required hydrogen for 200 miles as a function of fuel cell stack power	58

1.0 Introduction

Powertrain modeling and simulation are now standard tools in advanced automotive design. Over the past few years many vehicle simulation software tools have been developed including Advisor, PSAT, Autonomie, and others [17][18]. They are now considered the state-of-the-field and are used extensively in advanced technology analysis studies and in vehicle design studies. Vehicle models are usually used in two types of vehicle studies: technology assessments or powertrain design studies.

Vehicle technology assessment studies often assess the performance, efficiency, and environmental impact of technologies through modeling. It is common to model equivalent platforms with a few different powertrain technologies and to make comparisons across the technologies on the basis of a set of performance metrics [22]. This type of assessment is limited in utility because it only shows a subset of possible designs. More comprehensive technology assessments are possible by simulating a full spectrum of vehicles to show where, within the design space, one technology exists relative to other technologies.

On the other hand, vehicle design studies are often performed through the integrated use of modeling and optimization. In most design studies, component sizes and/or control strategy parameters are optimized to achieve the highest vehicle-level efficiency while maintaining performance [15][16]. These studies lack real world utility because: 1) they have limited scope because they require extensive simulation time, 2) models are rarely connected to system-level design objectives and requirements, 3) in the real world vehicles are designed for many competing objectives, and 4) design objectives and constraints are rarely concretely known. More flexible tools are required that communicate Pareto-optimal fronts as opposed to rigid single objective optimized designs.

In this thesis, I present a study of design methods that utilizes custom vehicle models to communicate Pareto-optimal tradeoffs within and across technologies. The tools developed for this research are used to make cross-technology evaluations and to perform high-level vehicle design.

2.0 Vehicle Modeling

Vehicle modeling is at the core of this research and therefore it will be discussed in detail and validated against the state of the field. Three different vehicle technologies are used in this thesis: 1) battery electric vehicles, 2) hybrid electric vehicles, and 3) fuel cell hybrid electric vehicles. The following sections describe the vehicle models and their validation.

2.1 Models

Table 1 lists the platform assumptions that are assumed to be constant across all vehicle architectures and technologies. Literature-based mathematical powertrain modeling was performed in Simulink with initialization and post-processing performed in MatLab. Much of the research was directed towards the development and validation of the vehicle models. Like Autonomie or PSAT (vehicle simulation tools commonly used in automotive design) the models utilized quasi-static engine maps, motor maps, battery open circuit voltage and impedance curves, and fuel cell polarization curves to model each component and determine component losses. Many of the low-level system dynamics are not modeled, as the purpose was to identify system-level tradeoffs between component sizes, architecture layouts, fuels, and control strategies, and not to perform detailed design. Likewise thermal systems were not included in these models for the same reason. The models were created with scalable components with component masses scaled linearly with component power and/or energy.

Table 1 2013 Chevy Malibu platform assumptions

Parameter	Value
Frontal Area	2.59m ²
Coefficient of Drag	0.34
Coefficient of Rolling Resistance	0.008
Chassis Mass (without powertrain)	1000kg

The top level of each model contained driver, supervisory controller and vehicle plant subsystems. Driver accelerator and brake pedal positions were fed into the supervisory controller that determined how the driver request was met. The output of the supervisory controller included commands to all controllable components on the powertrain (motor controller, engine, dc/dc converter, transmission, etc). Each component within the vehicle responded to supervisory control commands and the vehicle reacted dynamically. Vehicle models were initialized by loading the drive cycle, scaling the components, and initializing all parameters. A post-processing file calculated the vehicle attributes over the drive cycle including acceleration times, and fuel and electricity consumption in charge-depleting or charge-sustaining modes.

The major components within vehicle models included internal combustion engines, hydrogen fuel cells, permanent magnet electric motors, and lithium-ion batteries. Engine and motor maps were modeled through speed-torque-efficiency maps while batteries and fuel cells were modeled through current-voltage polarization curves and internal resistance curves. Three engines were modeled: a spark ignition E10 gasoline engine, a spark ignition E85 gasoline engine, and a compression ignition B20 diesel engine.

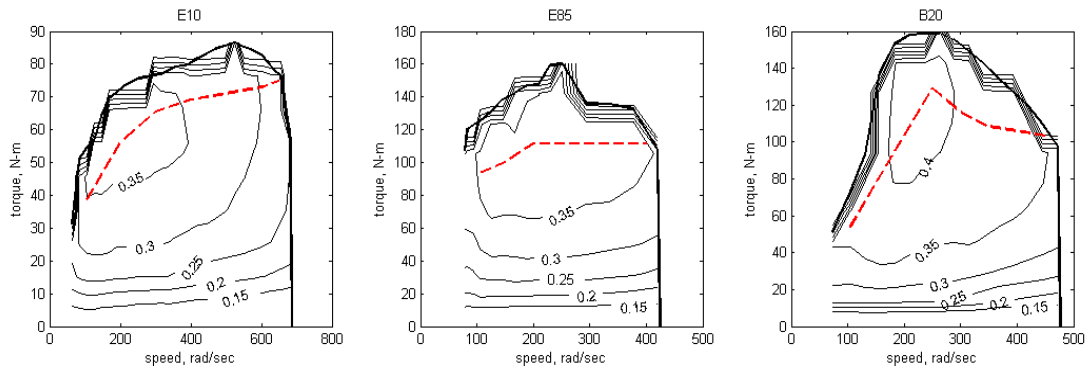


Figure 1 Efficiency maps and ideal operating lines for E10 (left), E85 (middle), and B20 (right) engines

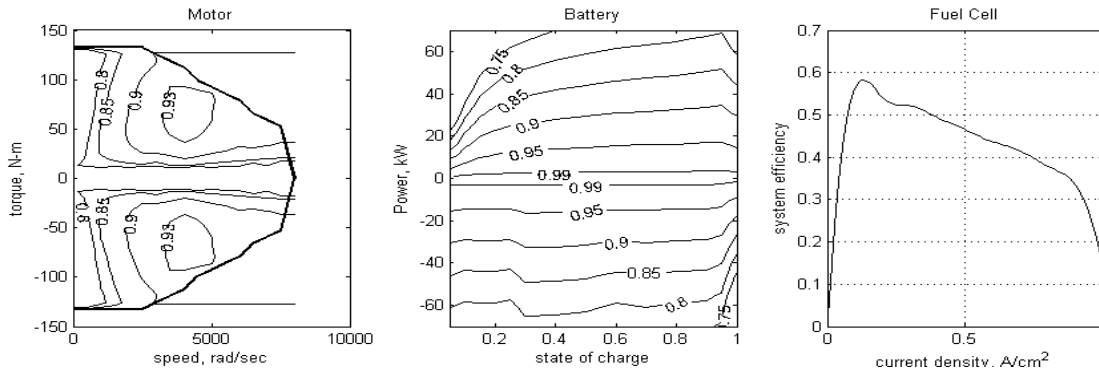


Figure 2 Efficiency maps for electric motor/generator (left), Li-ion battery (mid), and fuel cell system (right)

Initialization of vehicle models was performed in Matlab. In this step all component data were loaded and scaled and design rules were applied to initialize all parameters. As an example of a design rule, all transmission limits and gearing were defined so that engines and motors reached redline at the 100mph and engines reached idle at 5mph. This was in an effort to reduce the degrees of freedom of the design space while maintaining top speed equivalency across architectures.

The major components discussed above are the main sources of energy loss on the powertrain. Other sources of loss are assumed to be constant in vehicle simulations across vehicle platforms: auxiliary system losses (500 Watts), high voltage power electronics losses (95% efficiency), and transmission losses (95% efficiency).

The supervisory controllers for all architectures were designed to take advantage of the benefits of the respective architecture in an effort to ensure valid evaluations across technologies and architectures. Additionally, the control strategies were designed to operate consistently at a variety of component scales. In this way, the performance assessments of the vehicles remain valid with various component sizes.

In general, all vehicles were controlled so as to operate in both charge-depleting and charge-sustaining modes of operation. The continuous power unit(the IC engine or fuel cell) may be turned on through two mechanisms. The first is an energy request triggered by the battery state of charge management system, The second is a power request triggered when the battery and/or electric motor are not capable of meeting the driver power demand alone.

Parallel architecture PHEV supervisory controllers attempt to operate the engines on an ideal operating line (IOL) for energy management. To implement the IOL strategy, the engine power request was determined by the battery's deviation from its target SOC. The continuously variable transmission (CVT) was controlled to achieve an engine speed on the IOL to produce the desired power, while the engine throttle was controlled to stay on the IOL at all times. The engine can also turn on to assist in power requests, in which case it may deviate from the IOL when additional power is needed to meet the drive cycle. The engine is turned off and clutched out when it is not required or when the limits of the CVT prevent the engine from spinning within its operating speed range.

Series vehicles take advantage of the mechanically decoupled engine by operating at the engine's ideal operating point. If needed, the engine may also turn on for power requests when the battery is not capable of supplying sufficient power.

The fuel cell HEV supervisory controller operates the fuel cell in steady state at low power to achieve state-of-charge management. By operating at low power, the fuel cell efficiency is maximized and start-

ups are minimized. The fuel cell may also provide additional power when the battery is not capable of meeting the request alone.

2.2 Model Validation

Validation of these custom vehicle models was performed against Autonomie because it is a well validated vehicle simulation tool and is considered by many to be the state of the field. The sections below discuss electric vehicle, hybrid electric vehicle, and fuel cell hybrid vehicle validation against Autonomie on the US06 drive cycle.

The models are considered valid if the platform losses are identical to Autonomie, and the total energy consumption is reasonably close to the Autonomie model (considering they have different component efficiency maps and control strategies). The validation results are presented the following sections.

2.2.1 Electric Vehicle

Figure 3 shows the cumulative energy loss from each component of the powertrain. The dotted line is the Autonomie model and the solid line is the custom model being validated. From the figure it is clear that the inertia of the vehicle, the aerodynamic losses, and the tire losses are identical. Other component losses such as the motor and internal battery losses are similar but not identical. Figure 3 verifies that the custom model behaves very similarly to Autonomie for identical platform losses.

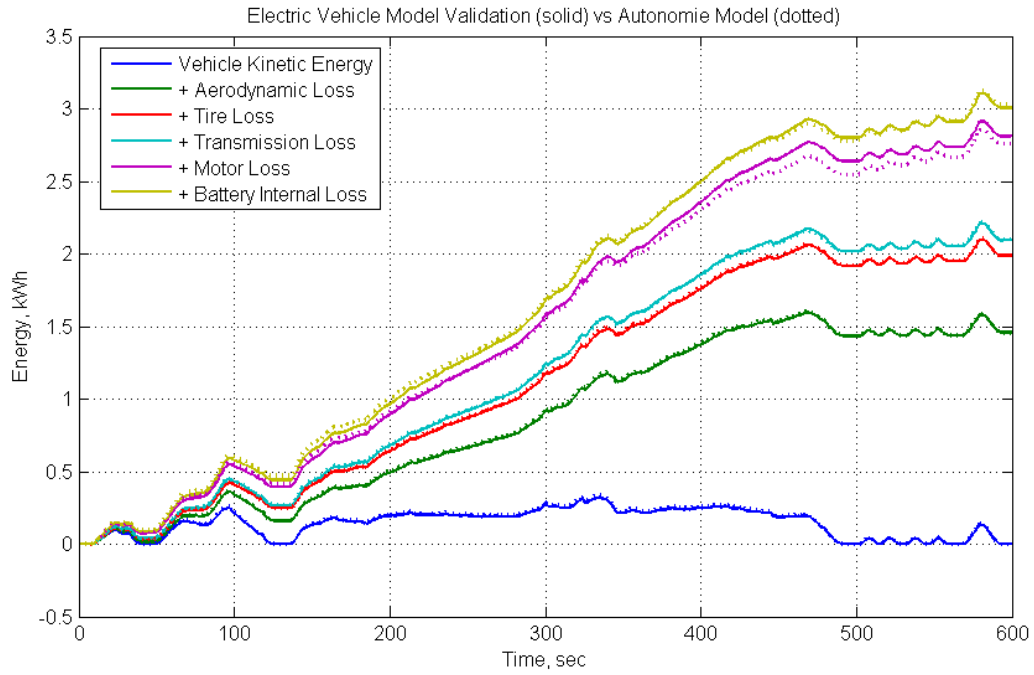


Figure 3 BEV energy loss validation on US06 cycle vs Autonomie

Figure 4 verifies that the vehicle speeds match the profile and the battery power is nearly identical for both the modeled BEV and Autonomie's BEV model. Through these figures, the BEV model is shown to be validated.

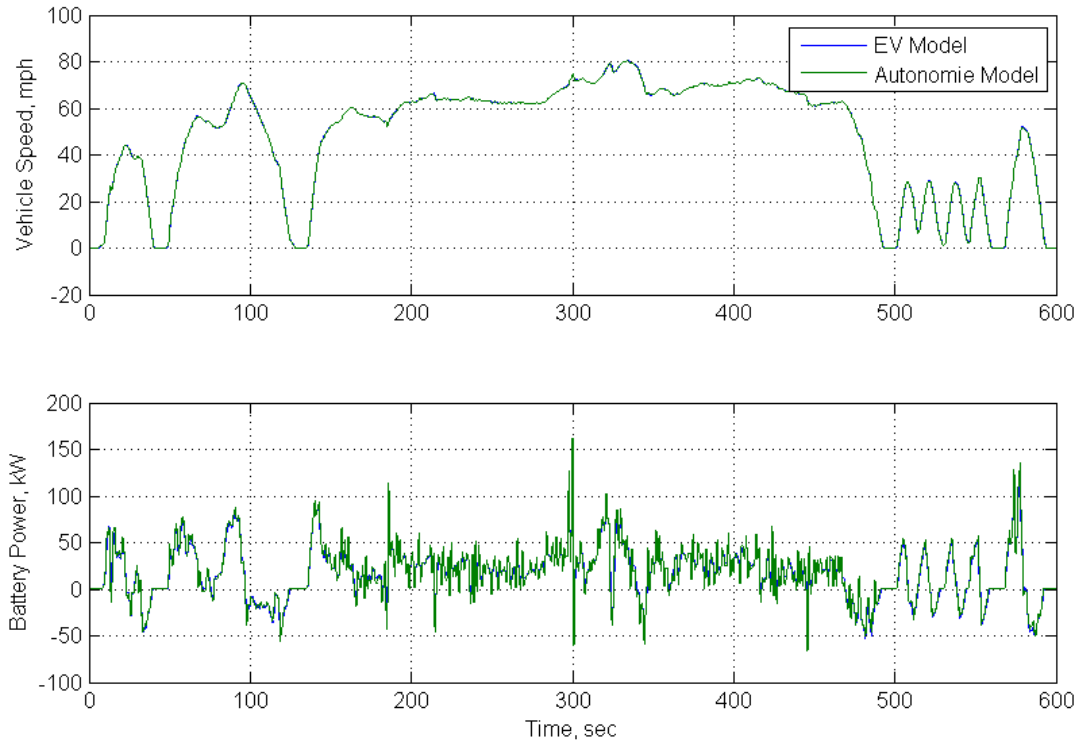


Figure 4 BEV simulation validation on US06 cycle vs Autonomie

2.2.2 Parallel Hybrid Electric Vehicle

The same validation effort can be considered for the parallel hybrid electric vehicle. It is clear from Figure 5 that the platform losses are identical between Autonomie and the custom HEV model. Different transmission, motor, battery, and engine losses are seen for two reasons: 1) the modeled subsystems have different efficiency maps, and 2) they are controlled differently. But the total energy consumption, seen in Figure 5, is very close to Autonomie. Therefore by the specified validation criteria the HEV model is validated.

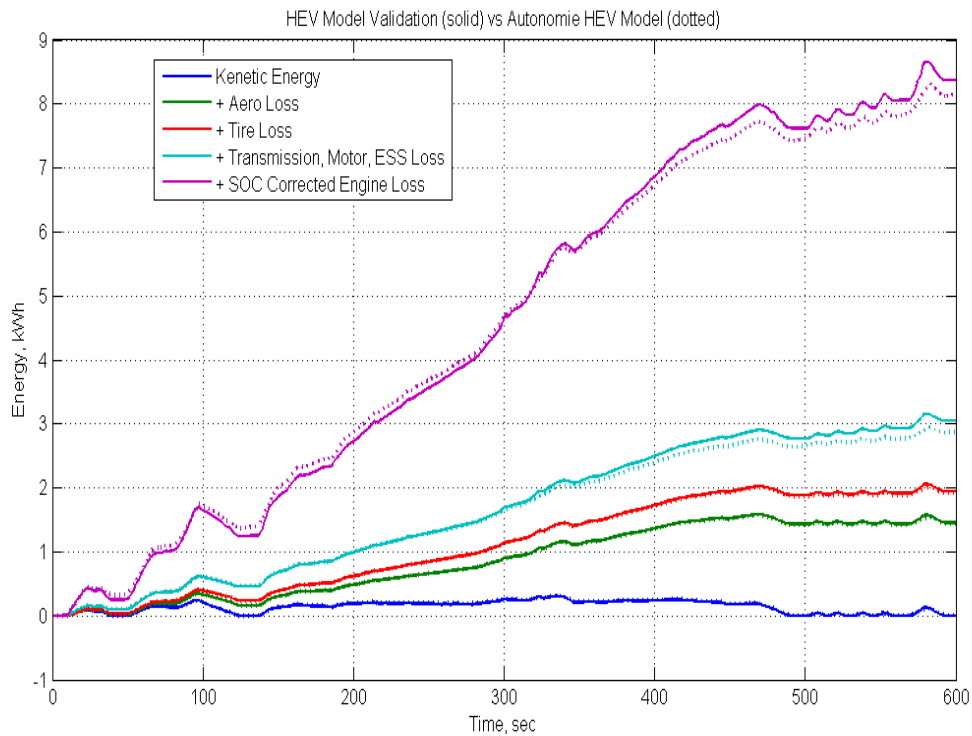


Figure 5 Parallel HEV energy loss validation on US06 cycle vs Autonomie

One notable difference between the models is seen in Figure 6 where the engine in the Autonomie model cycles on/off much more frequently. This is Autonomie's attempt to minimize losses from over use of the energy pathway from the engine into the battery. This control strategy difference is likely why Autonomie has slightly lower motor, transmission, and battery losses and slightly lower total energy consumption even though the engine's average efficiency is the same (35.5% efficiency). Through optimized controls, the custom model could probably achieve 3-5% better fuel economy.

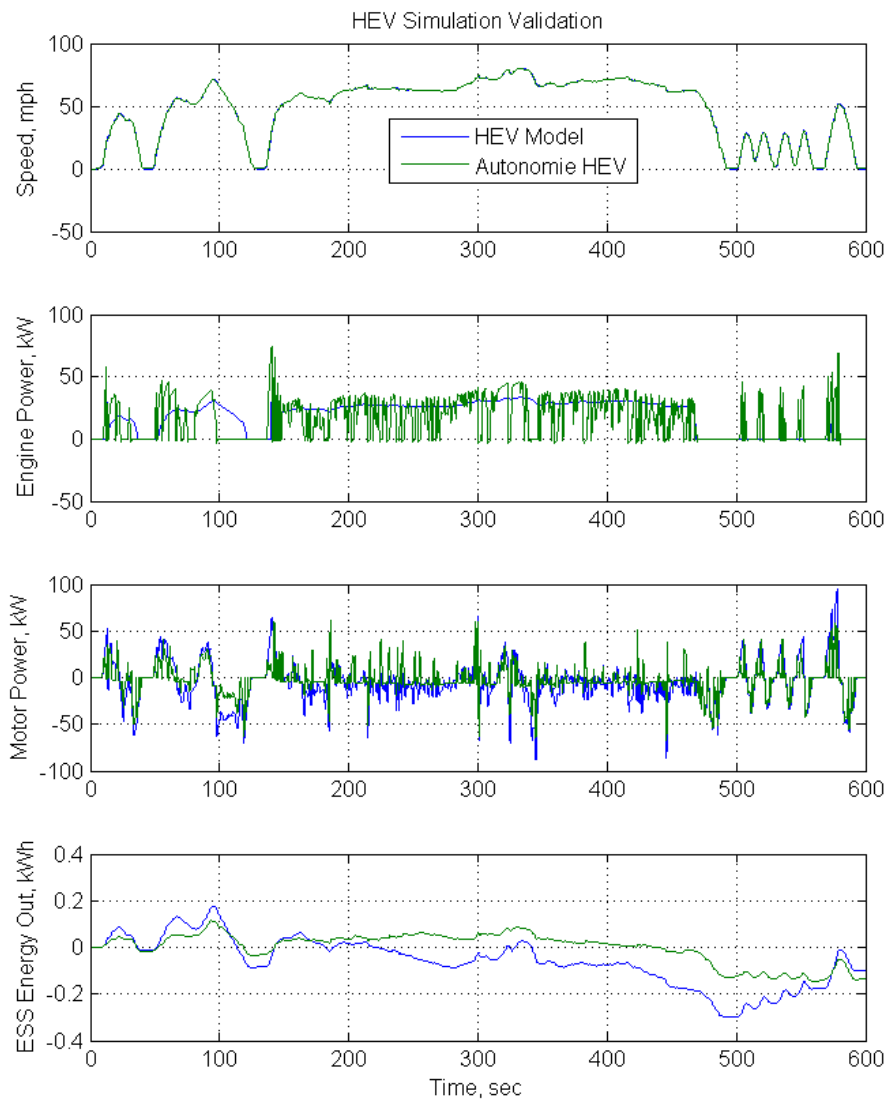


Figure 6 Parallel HEV simulation validation on US06 cycle vs Autonomie

2.2.3 Fuel Cell Hybrid Electric Vehicle

The same validation effort can be considered for the fuel cell hybrid electric vehicle. Figure 7 shows that the total energy consumption differs between Autonomie and our model, but the platform losses are identical. The transmission, motor, DCDC, and battery losses are very similar which indicates that the difference in total consumption is due to differences in fuel cell system efficiency. The models, however, do exhibit similar net energy consumption and identical platform losses, which by the specified criteria validates the Fuel Cell HEV model.

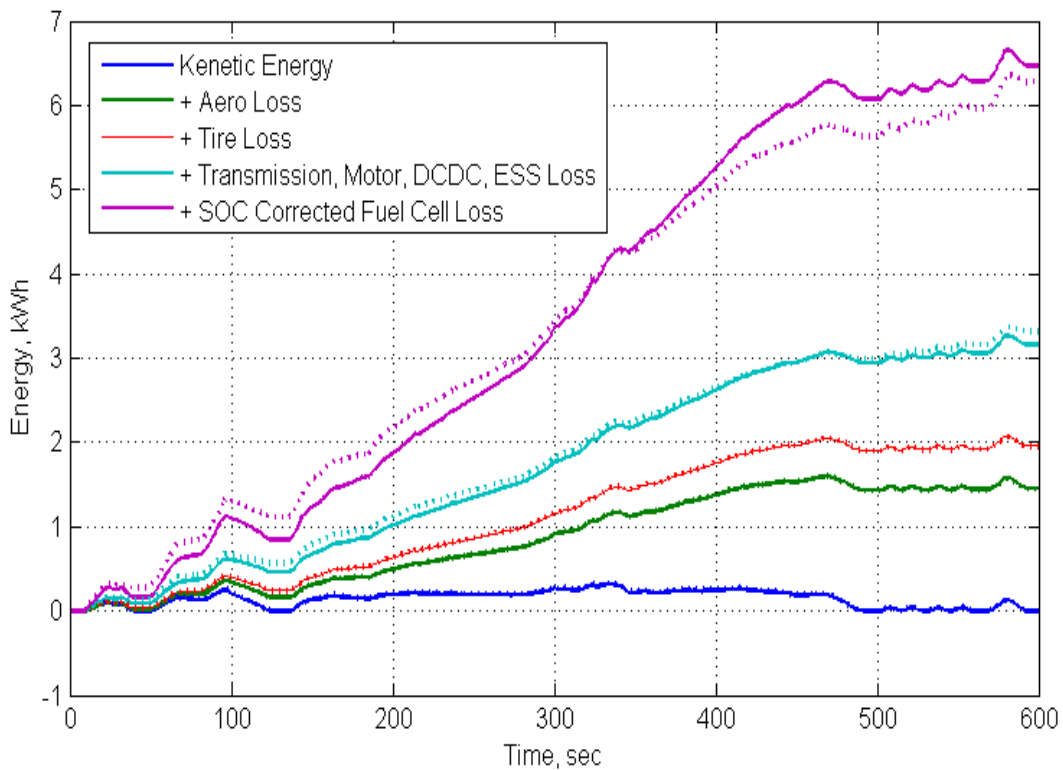


Figure 7 Fuel Cell HEV energy loss validation on US06 cycle vs Autonomie

Like the HEV model, Autonomie's Fuel Cell HEV model shows much more frequent on/off cycles of the fuel cell, as shown in Figure 8. Again, this is an attempt to minimize the use of the series fuel cell to battery energy pathway, which leads to higher losses. Optimized energy management controls could improve overall consumptions slightly.

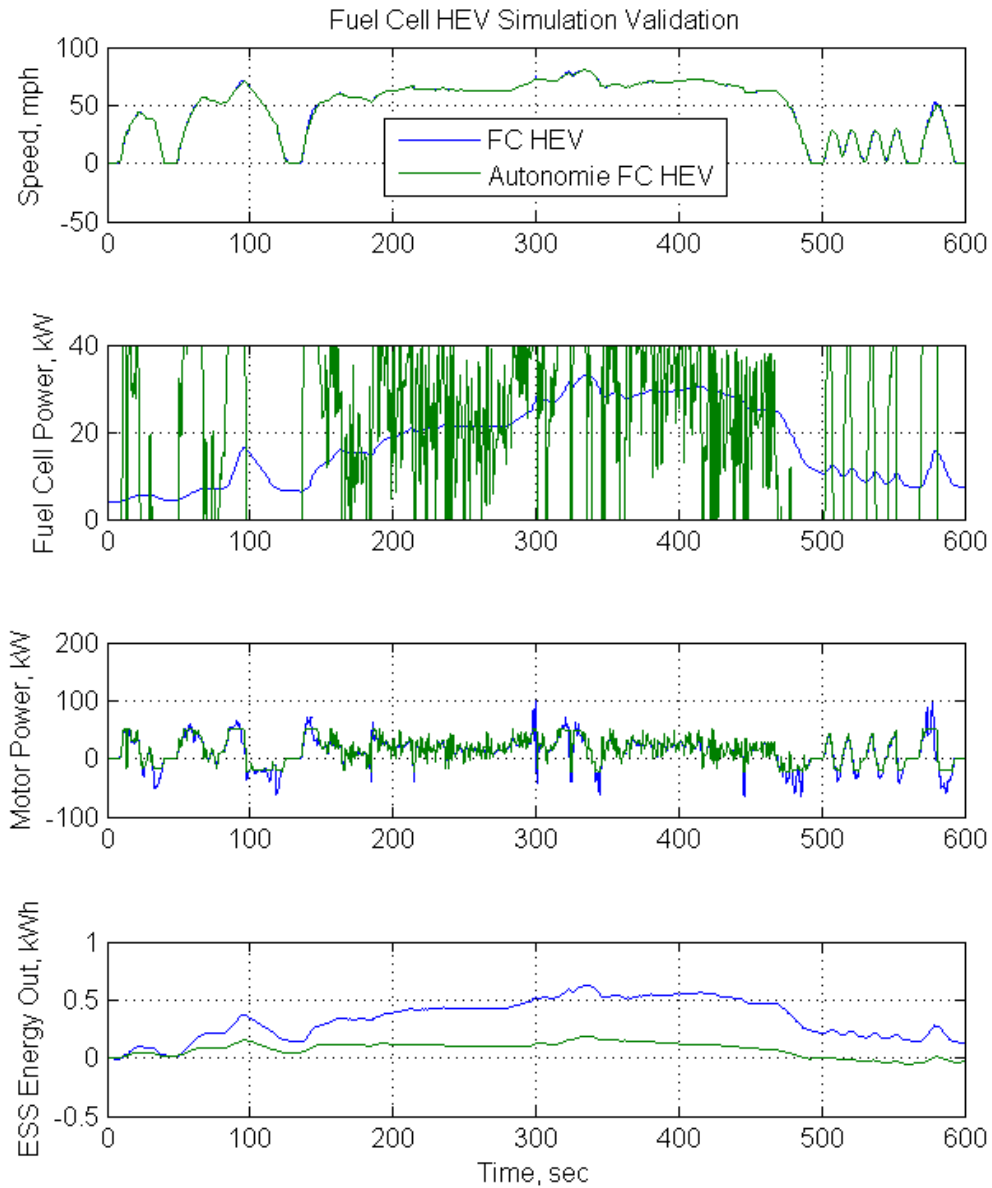


Figure 8 Fuel Cell HEV simulation validation on US06 cycle vs Autonomie

2.3 Conclusion

This section has presented the modeling system used for these investigations and has presented its validation against state of the art vehicle fuel economy and energy consumption models. The primary reason for developing custom models is to have the ability to programmatically implement the models in any type of study, whether it is a single simulation, a design optimization, or a design of experiments conducted serially or in parallel. The long CPU time and inability to separate the models from the cumbersome GUI were both reasons to avoid using Autonomie. Despite these deficiencies, Autonomie does serve as a benchmark on which to validate our custom modes. A comparison of CPU times between our custom model and for Autonomie is shown in Table 2. On average Autonomie requires an order of magnitude more time to complete a simulation due largely to the added pre-processing and post-processing time required by the GUI.

Table 2 Comparison of Autonomie vs. Custom model on the basis of CPU time for 505 cycle

	BEV	HEV	FC HEV
Autonomie CPU time (sec)	40.1	80.6	50.6
Our Model CPU time (sec)	4.3	9.3	4.9

3.0 Plug-in Fuel Cell Vehicle Technology and Value Analysis

In 2010, a study was performed to assess the value of a new, unexplored vehicle technology, plug-in fuel cell hybrid electric vehicles. The study was organized by the California Air Resource Board and the Electric Power Research Institute, and CSU was chosen to do the modeling analysis. The method was to have three advanced automotive experts each design a PFCV, CSU simulated these vehicles and evaluated them on several metrics. These three vehicles were then compared against some other promising advanced vehicle technologies: PHEVs and BEVs [4].

In fall 2011, the study was re-visited at CSU with a different modeling approach. Using models developed at CSU and presented above, a large number of PFCV designs was investigated with varying component sizes. This design-of-experiments led to a broader look at the PFCV technology as it relates to PHEV and BEV technologies, and illustrated PFCVs as a “technology bubble” as opposed to a few data-points. I argue that this approach to technology evaluation is a more comprehensive way to look at the feasibility of technologies. This argument is supported through the following paper which was published in EVS26, 2012. The paper shows that by looking at a broader spectrum of designs within each technology a big-picture view can be communicated. When looking at only a few data-points, the big picture is absent. In addition to gaining a view of the technology as a whole, a deeper understanding of the technology is gained by communicating the tradeoffs that exist within the technology as component sizes are varied. The following sections describe this study in detail.

3.1 Abstract

Plug-in Hydrogen Fuel Cell Hybrid Electric Vehicles (PFCVs) offer reduced operating and manufacturing costs when compared to conventional hydrogen fuel cell hybrid electric vehicles (FCVs) because they have downsized onboard fuel cells with improved range and refueling times when compared to grid-charged Battery Electric Vehicles (BEVs). As such, PFCVs provide opportunities to combine the advantages and mitigate the limitations of both FCVs and EVs. Although the PFCV concept has been

presented conceptually in the past, no quantitative analyses of its prospective technical, environmental, and economic characteristics have been performed until recently. Motivated by the basic promise of a new, high-efficiency, zero consumer compromise, and zero-emission vehicle, the authors have conducted an initial assessment of PFCVs in comparison with FCVs, BEVs and internal combustion engine-battery hybrid electric vehicles (PHEVs). This study was coordinated by the Electric Power Research Institute (EPRI) and supported by the California Air Resources Board (CARB) and the Southern California Air Quality Management District (SCAQMD). The study approach included the identification of representative PFCV, FCV, BEV and PHEV vehicle configurations, the modeling of these configurations, and the determination of their energy use, well-to-wheel carbon dioxide emissions, and cost characteristics. Results show that, with economies of scale, PFCVs can offer a competitive alternative to conventional PHEVs with the added benefits of being 100% petroleum independent and having zero tailpipe emissions. Within the context of PFCVs, a wide range of design freedom is possible. This study examines a wider range of possible designs, which suggest that low power fuel cells and high energy batteries provide benefits for environmental and cost metrics. The optimal vehicle here can be described as a hydrogen fuel cell, hybrid electric, range-extending vehicle (FCEREV).

3.2 Introduction

A plug-in fuel cell vehicle is an advanced technology electric vehicle concept with promise to help achieve key environmental and energy-strategic goals. In addition to being a zero-emission vehicle, the plug-in fuel cell vehicle combines the advantages of hydrogen fuel cell vehicles with those of grid-charged Battery Electric Vehicles (BEVs). It overcomes the range limitation and long refueling time of BEVs, considered by many to be the continuing barriers to their widespread acceptance. Compared to fuel cell vehicles, the plug-in fuel cell vehicle offers the customer lower fuel costs and home refueling with electricity from the grid. PFCVs offer the benefit of increased fuel cell operating efficiency while facilitating the market acceptance of FCVs in a phase of reduced availability of hydrogen infrastructure.

This ability promises to reduce the cost and increase the operating life of the fuel cell system, mitigating two of the most challenging issues faced by fuel cell vehicles.

Despite these potential advantages, the plug-in fuel cell vehicle has attracted little attention and detailed system-level analyses of the plug-in fuel cell vehicle have not yet been published [1][2][3][4]. As a consequence, it is not clear how the attributes of plug-in fuel cell vehicles compare with those of the most promising advanced vehicle technologies. Credible answers to these questions are needed before the potential of the plug-in fuel cell vehicle as an advanced electric technology vehicle option can be assessed.

3.3 Background

In 2011, a Phase 1 analysis of the technical, environmental and cost characteristics of three representative PFCV configurations and similar-sized FCVs, BEVs and PHEVs, currently the leading advanced electric technology vehicles, was conducted [4]. Six vehicles were selected in the Phase 1 study to represent a range of production and research passenger vehicles based on a sedan-sized platform (~1800kg). Coordinated by the Electric Power Research Institute on behalf of the California Air Resources Board and the California South Coast Air Quality Management District, the Phase 1 study was conducted by an international team of experts in advanced technology electric vehicle design, development, demonstration and assessment, and supported by expertise in vehicle modeling. State-of-the-art simulation techniques were used to determine and compare vehicle performance, driving range, energy consumption, operating costs, and Well-to-Wheels (WTW) carbon dioxide equivalent (CO₂-eq) emissions for representative driving cycles.

The conclusions of the Phase 1 study demonstrated a set of comparisons among PFCVs, FCV, BEVs and PHEVs on the basis of environmental and economic metrics. Graphic comparisons of the seven representative vehicles' updated simulation of WTW GHG emissions (using both California and U.S.

electricity mixes) as well as near- and long-term fuel costs are shown in Figure 9 and Figure 10 respectively.

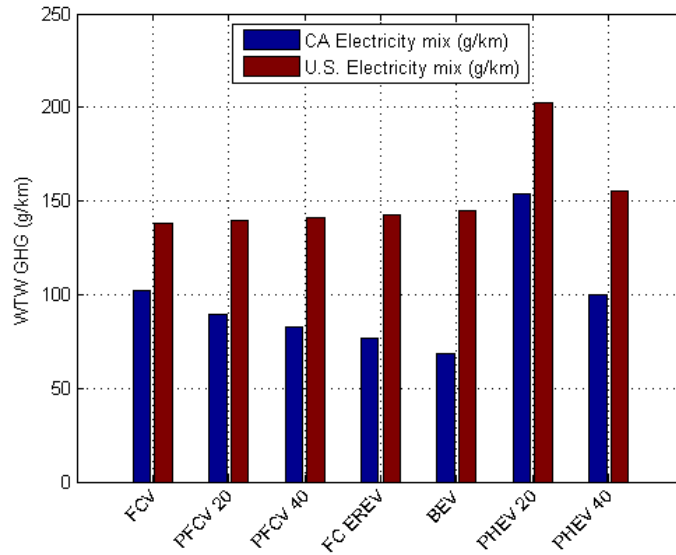


Figure 9 U.S. and California electricity mix WTW GHG emissions comparison for seven representative vehicles from Phase 1 study.

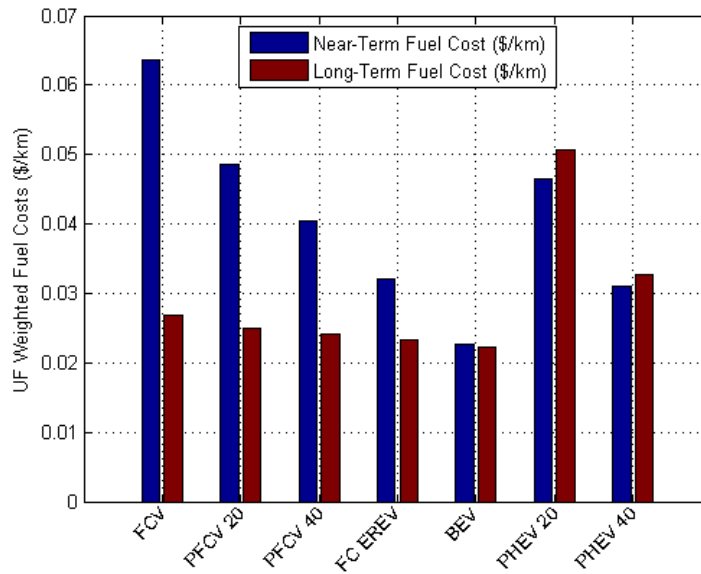


Figure 10 Near- and long-term fuel costs comparison for seven representative vehicles from Phase 1 study.

These results formed the motivation for an additional investigation of the design space encompassing PFCVs. Three goals were outlined for additional work:

- First, simulations performed for the previous results were subject to validation against expert opinion of theoretical performance. Additional analysis should provide a benchmark for simulation results against production advanced technology vehicles.
- Second, these results showed that increased battery energy (and thus increased CD range and AER) combined with fuel cells can be used to construct vehicles whose benefits increase with increased electrification. Additional analysis should define whether this trend continues by investigating a broader design space.
- Third, these studies were based on a set of vehicle designs defined by a committee of experts. It is unknown whether these designs are in fact representative of the performance characteristics of a particular vehicle technology (PFCV, PHEV, and BEV). Additional analysis should characterize the design space in more detail and should suggest Pareto-optimal design trends.

To expand upon the progression of vehicle designs towards increased electrification, the study presented in this paper provides additional analysis of the design space for BEVs, PHEVs, and PFCVs. The methods used for defining the vehicle architectures, models, simulations, and evaluation metrics are described in the following sections. Various results are presented to demonstrate a comparative benchmark, and a characterization of the design space with increased breadth and detail. Discussion and conclusions focus on the ramifications of this work for further study of the characteristics of PFCVs.

3.4 Methods

Vehicle models and simulations have been developed to represent state-of-the-art hybrid architectures. The methods of formulating a design of experiments (DOE), determining vehicle components, simulation, and results analysis are outlined in the following sections.

Two literature-based mathematical vehicle models were developed in Matlab/Simulink for this study: a plug-in hybrid electric vehicle with a conventional internal combustion engine, and a hydrogen fuel cell plug-in hybrid electric vehicle; the BEV model is based on the PFCV model with the hydrogen system removed. Each model was constructed with state-of-the-art quasi-static engine maps, motor maps, fuel cell polarization curves, and battery maps. Vehicle mass is calculated by summing the masses of vehicle components.

3.4.1 Drive Cycles

The vehicle models were simulated on a combination of drive cycles which include the Supplemental FTP (US06 divided into city and highway segments), Urban Dynamometer Driving Schedule (FU505), and Highway Fuel Economy Driving Schedule (HWFET). The data from each simulated cycle is weighted and used to determine the fuel and energy consumption, performance, range, etc. The weight of each cycle is as follows: 14.1% US06 City, 28.8% FU505, 44.5% US06 Highway, and 12.5% HWFET. This combination of drive cycles is chosen to be more representative of U.S. driver behavior than the EPA's city/highway drive schedule and is therefore a better metric on which to evaluate vehicle designs.

3.4.2 Design Variables

A full-factorial design of experiments was performed on the PHEV, PFCV and BEV design spaces. Vehicle designs are characterized by three design variables for this study: total vehicle power (kW), battery energy capacity (kWh), and degree of hybridization. For a parallel architecture vehicle, like the modeled PHEVs, the total tractive power is the sum of the electrical and mechanical drivetrain powers. For electric drive vehicles, like the PFCV model, the total tractive power is the electric motor power rating. With this definition, a vehicle with DOH of one represents an electric vehicle while a DOH of zero represents a conventional vehicle. Finally, the batteries are sized so that they are capable of sourcing the electric motor's peak power draw. With these three design variables and sizing rules, all

drivetrain component sizes are defined. Table 3 shows the ranges over which each of these design variables were varied in the design of experiments.

Table 3: Ranges of design variables investigated for each of the vehicle architectures simulated.

	PFCVs	BEVs	PHEVs
Battery Energy (kWh)	5-30	15-45	5-30
Degree of Hybridization	0.2-0.9	1.0	0.2-0.9
Vehicle Power (kW)	80-180	80-180	80-180

3.4.3 Design Metrics

The selected analysis metrics allow for inclusion of economic, environmental, and consumer acceptability assessment. They include fueling cost, WTW greenhouse gas emissions and performance. Analysis metrics use best current practices for vehicle comparison studies [4] and for well-to-wheel CO₂ emissions calculations [6][7]. The analysis metrics used in this paper are based on low fidelity models that will be refined in future studies. Future work will include detailed analysis of a broader set of analysis metrics including infrastructure investment and projected manufacturing costs as well as detailed analysis of WTW energy use and emissions.

Consumer fueling cost is calculated on a utility-factor-weighted fuel use basis. Near-term (2012) and long-term (2020) electricity and gasoline prices are estimated from the 2012 Annual Energy Outlook [9]. Hydrogen near-term and long-term costs are estimated from DOE targets [10]. Electricity costs are determined from residential rates, assuming that a majority of charging will occur at a vehicle owner's home. The long term scenario assumes that the costs of gasoline, electricity and hydrogen evolve in different ways over a period of approximately 10 years: gasoline prices increase under the impact of resource competition; electricity prices remain relatively stable due to embedded capacity and the continued availability of off-peak power for battery charging; and costs of hydrogen production and transportation decline with economies of scale.

Table 4: fueling cost analysis conversion metrics

	Gasoline (\$/kWh)	Electricity (\$/kWh)	Hydrogen (\$/kWh)
Near-term (2012)	0.093	0.113	0.266
Long-term (2020)	0.107	0.111	0.089

REET was used to estimate upstream Greenhouse Gas (GHG) emissions from each fuel source. Both United States (U.S.) and California (CA) electricity mixes are used [11]. CA electricity has lower upstream GHG content due to its larger proportion of renewables and nuclear power. The CA electricity mix is estimated to be more representative of future generation emissions around the world as increased amounts of renewable energy are utilized. Hydrogen upstream GHG emissions assume 100% natural gas (NG) reformed hydrogen as NG is expected to be the feedstock for hydrogen production in the foreseeable future. Downstream GHGs are calculated from the carbon content of the fuel.

Table 5: GHG emissions analysis conversion metrics

	Gasoline (g/kWh)	Electricity (g/kWh)	Hydrogen (g/kWh)
PTW GHGs	261.0	0.0	0.0
WTP CA GHGs	60.2	343.0	369.1
WTP U.S. GHGs	64.3	721.4	402.1

Performance of each vehicle is approximated using a power-to-weight ratio (P/W). Vehicles with high P/W will have high performance while low performance vehicles have a low P/W ratio.

3.5 Results

Simulation of each vehicle within the design space, across architectures, yields data that has been analyzed to determine optimal vehicle design. Simulation results are intended to provide benchmarking to state-of-the-art production vehicles, increase the breadth of the investigated design space, and identify trends within the design space to locate optimal designs. They further present technology and value assessments across the simulated design space as well as in comparison with current production and previously investigated vehicles.

3.5.1 Vehicle Benchmarking

The intention of vehicle benchmarking is to show that each simulated technology performs within an acceptable error of existing production vehicles and therefore provide confidence in trends and tradeoffs identified in the results of this study. As such, the benchmark simulations do not represent the exact architecture and control of the selected benchmark vehicles. The benchmark vehicles are simulated using manufacturer component specifications applied to the models described in this study. The benchmarking vehicles are: GM Chevrolet Volt (PHEV), Nissan Leaf (BEV), and Honda FCX Clarity (FCV). Benchmark vehicle performance values have been obtained from certified EPA testing data.

Comparison of simulated and tested vehicle performance shows that simulated vehicles operate within 10% of commercially available vehicles on the basis of charge-depleting fuel economy, charge-sustaining fuel economy, and charge-depleting range. Figure 11 shows the benchmarking result with near-equivalent error across fuels, providing a fair comparison of vehicle technologies.

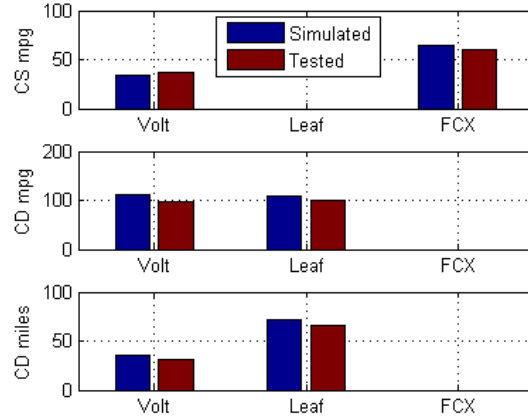


Figure 11 Benchmarking of simulations against commercially available vehicles

3.5.2 Increased Breadth of Design Space

The design variables investigated in this study cover a wide range of vehicle designs. Figure 12 shows all vehicle designs investigated, across architectures, along with the seven representative vehicles from the Phase 1 study. It can be observed in Figure 12 that the design space explored for this study greatly expands the breadth and detail of the design space simulated over the Phase 1 study.

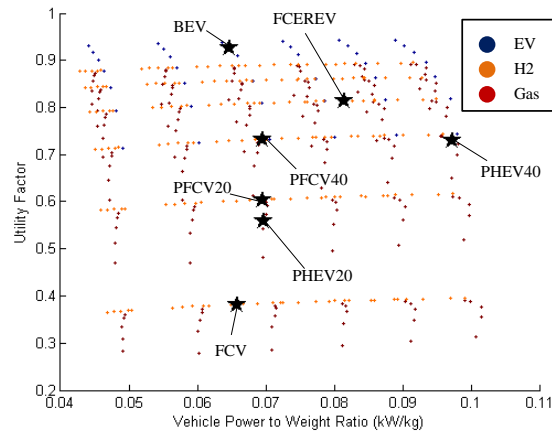


Figure 12 Vehicle design space power-to-weight ratio vs. utility factor.

Figure 13 and Figure 14 show “worst case” and “best case” vehicle design space evaluations respectively. U.S. WTW GHG emissions and near-term costs are considered a worst case for PFCVs due to high hydrogen costs and relatively dirty electricity generation. CA WTW GHG emissions and long-

term costs are more favorable for PFCV designs as CA offers more renewable energy sources (likely representative of future electricity generation) and are designated “best case”.

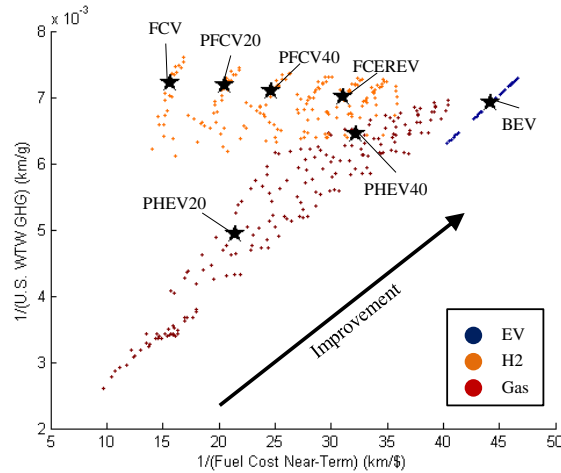


Figure 13 Vehicle designs near term fuel costs vs. U.S. electricity mix WTW GHGs, “worst case” scenario.

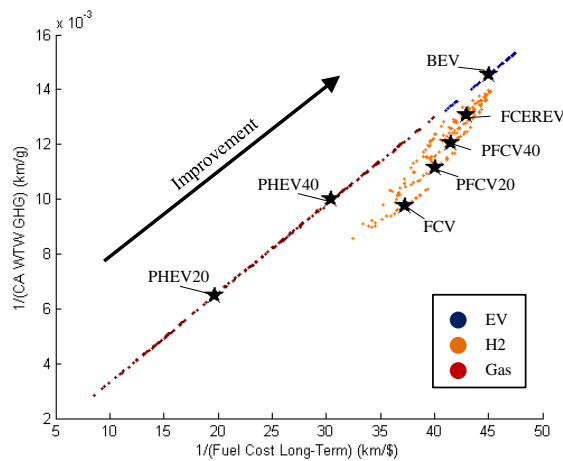


Figure 14 Vehicle designs long-term fuel costs vs. CA electricity mix WTW GHGs, “best case” scenario.

For each of the scenarios, it can be observed that BEVs minimize both fueling costs and WTW GHG emissions. Additionally, improved vehicle designs are available beyond the seven architectures investigated from the Phase 1 study. The existence of improved vehicle designs beyond the Phase 1

investigated vehicles suggests that further investigation of the design space should be performed to correctly characterize the potential of each vehicle technology.

3.5.3 Increased Vehicle Design Detail

Analysis of the simulated design space invites interest in the optimal vehicles represented. For each of the three-vehicle design variables (and for each of the three vehicle architectures) Pareto-optimal designs at each increment are determined based on the two analysis metrics (WTW GHGs and fueling costs). Pareto-optimal design fronts represent the non-dominated edge of the design space for the two analysis metrics, and can provide design tradeoff transparency to assist in vehicle design decision-making.

As mentioned, U.S. and CA electricity mix metrics are used in this study to compare different electricity generation scenarios. Figure 15, Figure 16, and Figure 17 show the WTW GHG emission based Pareto-optimal vehicle designs evaluated against DOH, vehicle power, and battery energy capacity respectively. For the CA scenario, BEVs offer the lowest WTW GHG emissions across all design variables. PFCVs offer slight improvements over BEVs and PHEVs for some U.S. WTW GHG based vehicle designs as hydrogen is leveraged by CO₂ intensive electricity generation. Increased use of hydrogen is preferable over electricity for low DOH and low energy capacity PFCVs. Figure 15, Figure 16, and Figure 17 show Pareto-optimal PFCVs as having lower emissions than Pareto-optimal gasoline PHEVs across all design variable ranges.

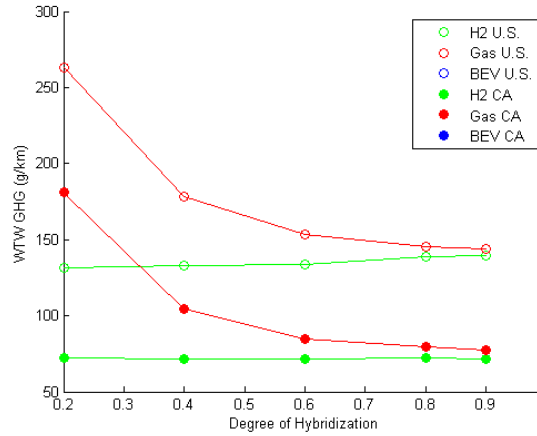


Figure 15 Pareto-optimal vehicles for U.S. and CA GHG emissions, by degree of hybridization.

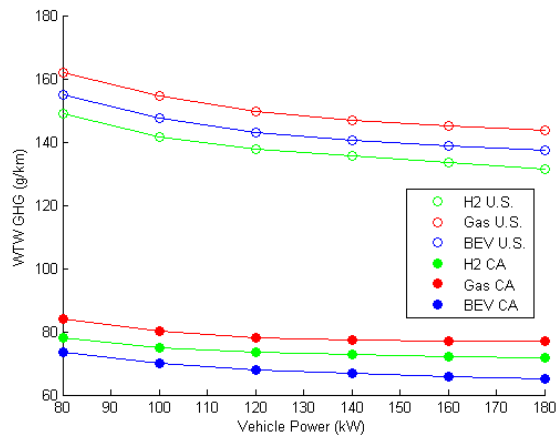


Figure 16 Pareto-optimal vehicles for U.S. and CA GHG emissions, by total vehicle power.

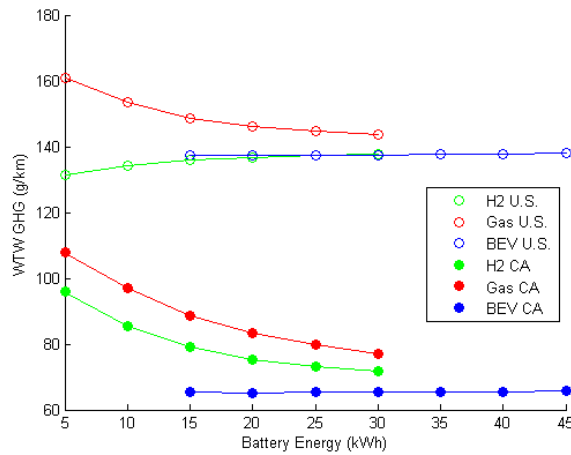


Figure 17 Pareto-optimal vehicles for U.S. and CA GHG emissions, by battery energy storage capacity.

Fueling cost scenarios for 2012 (near term) and 2020 (long term) have been used to evaluate the costs that consumers would incur on a per-kilometer basis assuming driving patterns similar to the four cycles listed in Section 0. Near-term and long-term Pareto-optimal vehicle designs are shown in Figure 18, Figure 19, and Figure 20 for each of the three fuels investigated. BEV's show the lowest fueling costs for all of the observed cases, followed by long term PFCVs and then near and long term PHEVs. PFCVs have the highest near-term fueling cost per kilometer due to high hydrogen costs in 2012. Fueling costs converge towards the fueling costs of BEVs as electrification increases.

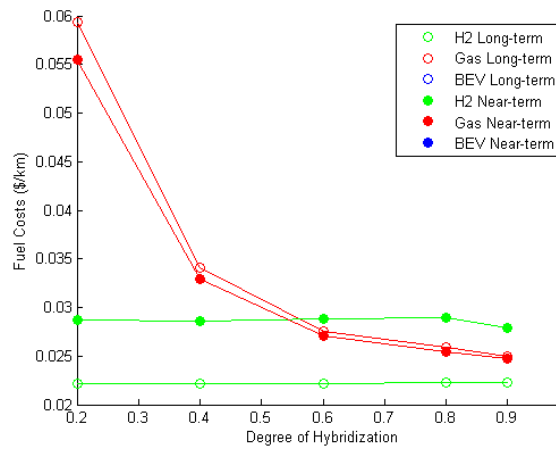


Figure 18 Pareto-optimal vehicles for near term and long term fuel costs, by degree of hybridization.

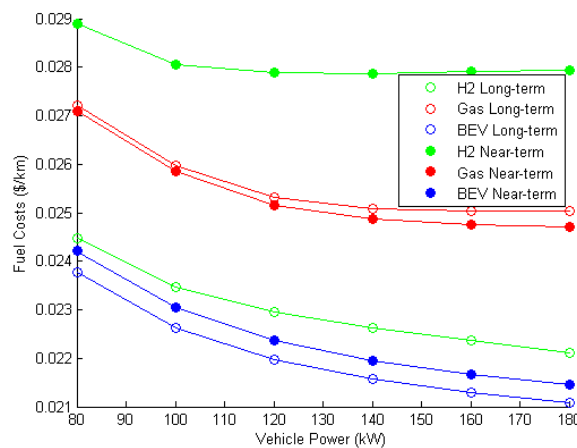


Figure 19 Pareto-optimal vehicles for near term and long term fuel costs, by total vehicle power.

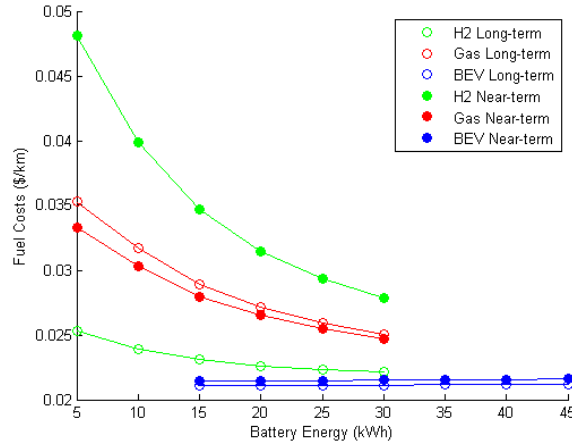


Figure 20 Pareto-optimal vehicles for near term and long term fuel costs, by battery energy storage capacity.

3.6 Discussion

The results of the design space exploration for PFCVs, BEVs, and PHEVs show the strengths of increased electrification with regard to WTW GHG emissions and fueling costs in all scenarios simulated. Investigation of Pareto-optimal vehicle designs reveals that all exhibit high power-to-weight ratios suggesting desirable driving responsiveness. Although BEVs show the lowest emissions and fueling costs for a majority of the observed vehicle designs, they suffer from reduced total driving range and long refueling times when compared to PFCVs and PHEVs. The leading vehicle design for each fuel type is displayed in Table 6.

Table 6 Leading BEV, FC-EREV, and ICE-PHEV design comparison.

	BEV	FC-EREV	ICE-EREV
Battery Energy (kWh)	20	30	30
Degree of Hybridization	1.0	0.9	0.9
Vehicle Power (kW)	140	180	180
Near-term fuel cost (\$/km)	0.0219	0.0279	0.0247
Long-term fuel cost (\$/km)	0.0215	0.0222	0.0250
U.S. WTW GHG (g/km)	140.45	139.44	143.71
CA WTW GHG (g/km)	66.77	71.66	77.09

For the leading vehicles, the BEV shows the most desirable performance. The PFCV and PHEV offer tradeoffs in costs, with the PFCV offering lower emissions. Both the leading PFCV and PHEV designs are characterized by high degrees of hybridization (0.9) and large battery capacity (30kWh), demonstrating that the most desirable PFCVs and PHEVs can be characterized as EREVs.

PFCVs show potential to offer low WTW GHG emissions, low refueling costs, and comparable dynamic performance in comparison with optimal BEV and PHEV designs. The benefit of PFCVs over comparable performance BEVs or PHEVs is an increased renewable energy use potential without sacrificing total driving range, performance, or refueling times. These results are consistent with conclusions from the Phase 1 study.

3.7 Conclusions

This paper has provided increased breadth and detail for three vehicle architecture design spaces. Analysis of the technology-specific design trends concludes:

- Vehicle benchmark simulations have provided proof of prevalent and accurate technology representations that are closely matched with production vehicle tested performance.
- Additional vehicle designs beyond those observed in the Phase 1 study can offer increased benefits, dominantly when applying increased electrification.
- Diminishing returns on WTW GHG reduction and fueling costs exist at very high battery energy capacity vehicles, particularly above 30kWh. This trend suggests that the correct breadth of the design space was investigated.
- In the near term, PFCVs can be expected to cost substantially less to operate than FCVs.
- Over the longer term, hydrogen and gasoline prices are expected to converge, allowing highly efficient hydrogen use in fuel cells to offer reduced consumer fueling costs.
- When charged with “low-CO₂” electricity, mid-size PFCVs cause substantially lower well-to-wheel greenhouse gas emissions than FCVs, with EVs, FC-EREVs and ICE-EREVs producing the lowest emissions.

Taken together these conclusions indicate that PFCVs could increase the acceptance and accelerate the introduction of fuel cell-powered vehicles. PFCVs promise lower operating costs and reduced well-to-wheels releases of CO₂. PFCVs also offer potential for increasing the penetration of electricity in transportation in the longer term because they overcome the limited driving range and long recharge times of EVs with little increase in operating costs.

4.0 Technology Assessment and High-Level Design Optimization for EcoCAR2

Section 0 described a case study in which a broader approach to technology assessment was taken to gain a big-picture view of the technology as it relates to other promising technologies. This study also gave some insight into design tradeoffs within the technology itself. In 2011, a more sophisticated tool was developed to evaluate technology, perform high level vehicle design, and to enable communication to decision makers. This “decision support tool” was demonstrated on CSU’s EcoCar2 vehicle architecture selection and is presented in the following sections. The paper was published in IECEC/JPC in August, 2012 [20]. In this thesis, I argue that the use of an interactive decision support system that integrates vehicle simulations that are efficiently optimized on system level design metrics is more effective when assessing technologies and performing high level vehicle design. This hypothesis is supported by the following paper which illustrates that CSU’s EcoCar2 design will mathematically dominate other competition vehicles on the basis of the design objectives laid out in the EcoCar2 rules.

4.1 Abstract

Modeling and simulation are becoming standard tools in the academic and industrial worlds of advanced automotive design. When coupled with optimization, these tools have the potential to fundamentally change the design process and facilitate rapid progress in the state of the field by enabling the use of inverse design methods

In inverse design, the designer controls decision variables directly, and design variables are obtained as outputs. Through inverse design, the tradeoffs imbedded in vehicle technologies can be communicated efficiently to decision makers. The full capabilities of inverse design, however, have not yet been realized due to lengthy simulation run times for optimization and a lack of models integrated with the decision metrics. As first-time participants in the EcoCAR2 competition, the Colorado State

University design team embarked on a research mission to investigate feasible technologies and identify tradeoffs within the context of the competition, which required confronting these roadblocks.

To perform architecture selection and component sizing, the CSU team developed a decision support system (DSS) from which inverse design was performed. Surrogate models of the vehicle design space were developed to reduce computation time, and competition-relevant decision metrics were directly integrated to enable inverse design. This unique approach enabled the evaluation of optimized technology options within the context of the competition and provided for the assessment of Pareto-optimal tradeoffs within each technology option. With this tool, we explored the design space of the EcoCAR2 competition and selected a vehicle architecture that, if executed properly, will dominate other competition vehicles. The CSU design team has chosen to build a blended charge-depleting mode plug-in fuel cell hybrid electric vehicle that optimizes energy consumption and emissions while meeting consumer acceptability requirements. The methods and results of this research are presented in the following report.

4.2 Introduction

EcoCAR2 is a three-year plug-in hybrid electric vehicle design/build competition funded by the US Department of Energy and General Motors in which fifteen universities are selected to compete. The technical goal of the competition is to reduce the energy consumption and emissions of a 2013 Chevrolet Malibu without compromising performance, utility, or safety [12]. As first time participants, the Colorado State University design team carried out an investigation into feasible architectures and component sizes. The goals of the research were: first, to identify and communicate tradeoffs among vehicle architectures, fuels, and components; second, to select an innovative and futuristic vehicle design not typically explored by researchers or OEMs that achieves environmental and energy sustainability; and finally, to design a winning vehicle for the EcoCAR2 competition that reflects the team's vision of the future of

transportation sustainability. This research utilized state of the art engineering tools including vehicle modeling, simulation, and optimization, as well as surrogate model development to facilitate inverse design.

Within the constraints of the competition, a wide range of design freedom is available, leading to a large design space, and therefore to high computational costs when simulations are coupled with optimization. The computational costs become intractable when more advanced design tools, such as Pareto-optimal tradeoff analyses, are implemented. To circumvent the challenge of computation time, an interactive, simulation-integrated, decision support system (DSS) was developed by the CSU team using neural network surrogate models of the vehicle design space. The DSS was formulated as a multi-objective optimization problem where the user defines objective function weights and constraints, and can graphically explore the design space in real time.

The DSS presented in this report was used as a design tool from which tradeoffs were communicated and multi-criteria decision analysis was used to make design decisions. Using the DSS, the team was able to use an inverse design process to determine that a hydrogen fuel cell plug-in hybrid electric vehicle is the optimal technology for the CSU team's goals, and is likely to outperform other vehicles in the competition.

4.3 Methods

To circumvent the challenge of computation time, a surrogate modeling approach was taken. In this approach, vehicle modeling and simulations were performed to populate a database of feasible vehicle designs by using a full factorial design of experiments. The database was used to construct surrogate models, which represented the continuous design space of the vehicle models. A decision support system was constructed that accessed surrogate models and performed user-defined optimizations and tradeoff analyses, and graphically communicated the design space to the decision maker. One unique advantage to this approach was that the DSS enabled vehicle design to be conducted inversely. Rather

than selecting design variables (component sizes, fuel, and architecture, etc.), running simulations, and obtaining vehicle attributes, as is typically done in a forward facing design process, the designer defined vehicle attributes, ran high speed optimizations, and obtained the required design variables that produce the desired attributes.

The following sections describe in detail the methods used to construct the decision support system. The steps include vehicle modeling and simulation, database development through a design of experiments, surrogate model training and validation using neural networks, and the decision support system formulation and utilization.

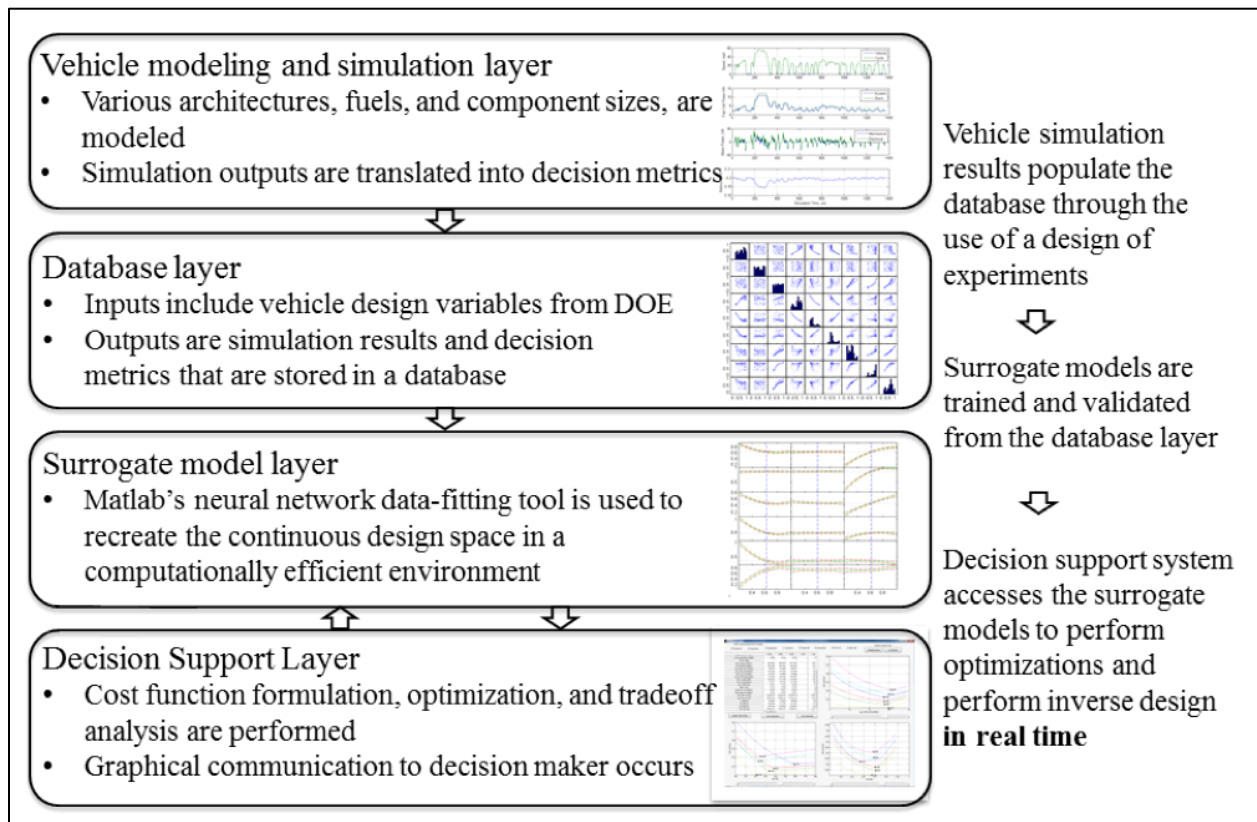


Figure 21 Decision support system data flow

4.3.1 Design Metrics

The vehicle models were simulated on a combination of drive cycles including the US06 divided into city and highway segments, the urban dynamometer driving schedule (FU505), and the highway fuel economy driving schedule (HWFET). The results from each cycle were weighted and used to determine the combined fuel and energy consumption, range, and other attributes. The weightings applied to the

results from each cycle were as follows; 14.1% US06 city, 28.8% FU505, 44.5% US06 highway, and 12.5% HWFET. This combination of drive cycles is designed to be more representative of typical US driver behavior than the EPA's city/highway drive schedule and is therefore a better environment in which to evaluate vehicles. Studies have shown that optimized vehicle designs differ depending on the drive conditions over which they were optimized, and therefore it is important to select the most representative drive cycles for the vehicle's application. This combination of cycles is also the combined drive schedule on which the EcoCAR2 competition evaluates vehicles.

Each vehicle was evaluated on several metrics including pump-to-wheel energy consumption (Wh/km), well-to-wheel petroleum energy use (Wh/km), well-to-wheel greenhouse gas emissions (g/km), well-to-wheel criteria emissions (bin), acceleration (sec), and gradeability (% grade). The metrics were calculated from simulation outputs on a utility-factor-weighted basis using the EPA standards and SAE best practices.

Outputs of simulations included the combined CD fuel use (g/km), CS fuel use (g/km), CD electricity use (Wh/km), CS electricity use (Wh/km), and CD range (km). Performance outputs such as 0-60mph acceleration time were obtained by simulating an acceleration test.

Argonne National Lab's GREET model was used for full fuel cycle emissions analysis under the approximation of mixed US and California marginal transportation electricity generation. The values obtained from GREET and used in the fuel cycle analysis are presented in **Table 8**. The fuel properties of each available fuel are presented in Table 7. The following paragraphs describe how each metric was calculated from the simulation results.

Table 7 Fuel properties

Metric	Unit	Fuel				
		E10	E85	B20	Elec	H2
Energy Density	kWh/kg	11.44	7.96	11.55	N/A	33.3
Energy Density	kWh/L	8.534	6.265	8.878	N/A	N/A

Table 8 Well to wheel analysis metrics

	Metric	Units	Fuel				
			E10	E85	B20	Elec	H2
Well to Pump	PEU	kWh/kWh	0.044	0.056	0.049	0.034	0.010
	THC	g/kWh	0.061	0.048	0.010	0.003	0.003
	CO	g/kWh	0.012	0.005	0.009	0.033	0.014
	NOx	g/kWh	0.028	0.014	0.021	0.101	0.032
	GHG	g/kWh	61.600	0.670	11.200	648.000	392.000
Pump to Wheel	PEU	kWh/kWh	0.940	0.260	0.810	0.000	0.000
	THC	g/kWh	0.010	0.012	0.003	0.000	0.000
	CO	g/kWh	2.604	2.994	0.450	0.000	0.000
	NOx	g/kWh	0.098	0.113	0.118	0.000	0.000
	GHG	g/kWh	261.000	260.000	277.000	0.000	0.000
	Fuel Cost	\$/kWh	0.093	0.107	0.093	0.113	0.266

The utility-factor-weighted pump-to-wheel energy consumption (Wh/km) was calculated from the CS and CD fuel and electrical energy consumption through the following equation:

$$EC_{Wh/km} = UF * (EC_{CD_{fuel}} + EC_{CD_{elec}}/eff_{charger}) + (1 - UF) * (EC_{CS_{fuel}} + EC_{CS_{elec}}/\sqrt{eff_{eng}/fc})$$

where EC is the energy consumption from either electricity or fuel (Wh/km), UF is the utility factor, $eff_{charger}$ is the charger efficiency (85%), and $\overline{eff_{eng/fc}}$ is the average engine or fuel cell to battery pathway efficiency. In this way, the energy consumption is calculated on a utility-factor-weighted and state-of-charge balanced basis.

The UF-weighted well to wheel petroleum energy use (Wh/km) was calculated from the upstream (well to pump) and downstream (pump to wheel) petroleum consumption. WTW PEU was calculated as follows:

$$PEU_{Wh/km} = UF$$

$$* \left(EC_{CD_{fuel}} * \left(PU_{wtp_{fuel}} + PU_{ptw_{fuel}} \right) + EC_{CD_{elec}} / eff_{charger} \right.$$

$$* \left(PU_{wtp_{elec}} + PU_{ptw_{elec}} \right) + (1 - UF) * \left(EC_{CS_{fuel}} + EC_{CS_{elec}} / \overline{eff_{eng/fc}} \right)$$

$$* \left(PU_{wtp_{fuel}} + PU_{ptw_{fuel}} \right)$$

where PEU is the total petroleum energy use (Wh/km) and PU represents the fraction of petroleum energy used per unit of energy consumed in the vehicle (kWh/kWh). PU upstream and downstream factors were derived from GREET and are presented in **Table 8**.

UF-weighted greenhouse gas emissions (g/km) were calculated by adding upstream and vehicle operation GHG emissions using the following equation:

$$GHG_{g/km} = UF$$

$$* \left(EC_{CD_{fuel}} * \left(GHG_{wtp_{fuel}} + GHG_{ptw_{fuel}} \right) + EC_{CD_{elec}} / eff_{charger} \right.$$

$$* \left(GHG_{wtp_{elec}} + GHG_{ptw_{elec}} \right) + (1 - UF) * \left(EC_{CS_{fuel}} + EC_{CS_{elec}} / \overline{eff_{eng/fc}} \right)$$

$$* \left(GHG_{wtp_{fuel}} + GHG_{ptw_{fuel}} \right)$$

where the upstream and downstream GHGs (g/kWh) were derived for each fuel using GREET and are presented in **Table 8**.

Similar to other metrics, the utility-factor-weighted well-to-wheel criteria emissions were calculated by adding upstream and vehicle operation criteria emissions. Criteria emissions include total hydrocarbons (THC in g/km), carbon monoxide (CO in g/km), and nitrogen oxides (NOx in g/km). The emissions were evaluated in a bin structure by determining the bin of each compound. The single criteria emissions value corresponded to highest, or worst, bin achieved. The criteria emissions bin structure is shown in **Table 9**.

Table 9 Criteria emissions bin structure

	THC	Nox	CO
Bin	g/km	g/km	g/km
10	0.078	0.373	2.610
9	0.078	0.186	2.610
8	0.056	0.124	2.610
7	0.056	0.093	2.610
6	0.056	0.062	2.610
5	0.044	0.043	2.610
4	0.043	0.025	1.305
3	0.034	0.019	1.305
2	0.006	0.012	1.305
1	0.003	0.006	0.652

Gradeability is the percent grade that the vehicle can climb for an infinite duration at 60mph. Rather than running time-intensive simulations, gradeability was approximated using basic vehicle dynamics. It was assumed that the continuous power unit (the IC engine or fuel cell) needed to provide all of the power on the gradeability test. Gradeability was calculated as follows:

$$\%Grade \approx \sin^{-1} \left(\frac{\frac{P_{cont}}{v} - \frac{1}{2} * \rho * A_f * C_d * v^2 - m * g * C_{rr}}{m * g}} \right) * 200/\pi$$

where P_{cont} represents engine or fuel cell power, A_f is vehicle frontal area, C_d is coefficient of drag, m is vehicle mass, and C_{rr} is the coefficient of rolling resistance.

4.3.2 Decision Support System

A full factorial design of experiments was performed on the available design space. Five design variables were investigated including vehicle architecture, fuel, battery capacity (kWh), degree of hybridization, and tractive power (kW). The three architectures were: series plug-in hybrid electric vehicles (Series PHEV), parallel plug-in hybrid electric vehicles (Parallel PHEV), and series fuel cell plug-in hybrid electric vehicles (Series PFCV). Four fuels were available to the competition including E10, E85, B20, and compressed hydrogen gas (in addition to grid electricity).

Added battery capacity increases the fraction of electrical energy on the drivetrain, which translates to increased charge-depleting range. Increasing the degree of hybridization raises the fraction of electrical power on the drivetrain, which translates to higher EV-only capabilities but lower continuous gradeability (due to reduced engine/fuel cell size). Lastly, the tractive power is the peak power that the vehicle can output at the wheels which can be directly translated to vehicle acceleration. With these design variable definitions, the EcoCAR2 design space was fully explored.

The full factorial design of experiments was performed for the 5 design variables and ranges shown in Table 10. Design variable ranges were defined based on available component size ranges. Each architecture alternative populated a design space with 175 designs that spanned all combinations of design variables within their defined ranges.

Table 10 Design of experiments variables ranges

Design Variable Name	Design Variable Range
Architecture	Series, Parallel, Series FC
Fuel	E10, E85, B20, H2
Vehicle Max Power	100, 120, 140, 160, 180kW
Degree of Hybridization	0.3, 0.4, 0.5, 0.6, 0.7, 0.8 ,0.9
Battery Capacity	5, 10, 15, 20, 25kWh

To perform multi-criteria analysis, the database was normalized. By normalizing the database each metric is made unit-less and of the same scale. It is beneficial to have metrics of similar scales when building multi-objective cost functions, as one metric is less likely to dominate the objective function. Normalization also ensures that surrogate models are fitted accurately as each input and output is considered equally important when they are of the same scale. Normalization was obtained through the following equations:

$$z_{norm} = \frac{z - z_{min}}{z_{max} - z_{min}} * 0.8 + 0.2$$

where:

$$z_{min} = mean(z) - 2 * std(z)$$

and:

$$z_{max} = mean(z) + 2 * std(z).$$

Each evaluation metric was normalized based on the statistics of the database while outliers did not dramatically influence the normalization. In this way, multi-criteria analysis and statistical modeling were enabled. This method is also similar to the way in which vehicles will be evaluated in the EcoCAR2 competition.

The normalized database was used to train and validate neural network surrogate models of the vehicle design space. The surrogate models were formulated using Matlab’s neural network data-fitting tool with 10 hidden nodes, which achieved acceptable correlation while not over-fitting the design space. In this way the interactions between design variables and decision variables were statistically modeled. The vehicle design space is recreated in a computationally efficient environment (networks are evaluated orders of magnitude faster than vehicle simulations). Table 11 shows the results of the neural network training and validation for each architecture. The results show that a regression value (R^2) of greater than 0.996 and mean squared error (MSE) of less than 0.000261 were achieved for all architectures, verifying that accurate surrogate models were achieved.

Table 11 Training and validation results from neural network fitting

	Samples	Hidden Nodes	Validation	Testing	MSE	R²
H2 PFCV	175	10	15%	15%	5.23E-05	9.99E-01
Parallel PHEV E85	175	10	15%	15%	3.48E-05	9.99E-01
Parallel PHEV B20	175	10	15%	15%	3.58E-05	9.99E-01
Parallel PHEV E10	175	10	15%	15%	2.77E-05	9.99E-01
Series E85 PHEV	175	10	15%	15%	2.77E-04	9.96E-01
Series B20 PHEV	175	10	15%	15%	2.61E-04	9.96E-01

The graphical user interface (GUI) of the DSS puts the design power in the hands of the decision maker and graphically communicates the design space. The user selects which architecture(s) to explore, defines objective function weights and constraints, runs optimizations and tradeoff analyses, and graphically explores the design space. A screenshot of the DSS GUI is shown in Figure 22.

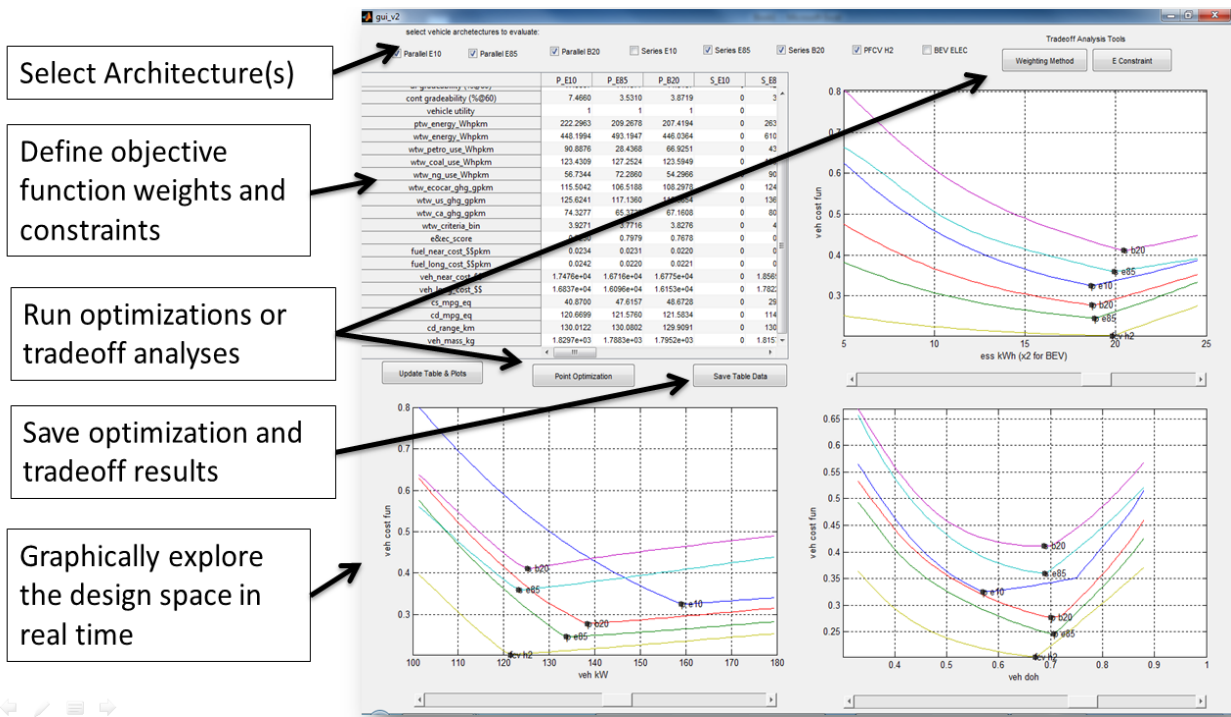


Figure 22 Decision support system user interface

4.4 Results

The DSS was used as a tool to perform analysis on the available design space of the EcoCAR2 competition. The mission of the competition is to reduce fuel consumption and emissions while maintaining consumer acceptability. These goals were integrated into the vehicle design process by adding them as optimization objectives and constraints. The results, using the inverse design process discussed previously, are presented in the following sections.

In the competition, vehicles are evaluated on four emissions and energy consumption metrics, which include WTW petroleum energy use (Wh/km), PTW energy consumption (Wh/km), WTW greenhouse gas emissions (g/km), and WTW criteria emissions (bin). In the competition, each metric is normalized with respect to competing teams and the normalized metrics are weighted equally and added to produce a composite “Emissions and Energy Consumption Score”. Utilizing the same approach, a cost function was created that represents the EcoCAR2 Emissions and Energy Consumption (E&EC) Score. The consumer acceptability metrics such as acceleration and gradeability can be thought of as constraints

on the design space and are formulated as such in the optimization. Therefore, the architecture selection and component sizing can be formulated, using this DSS, as an optimization problem where the EcoCAR2 E&EC score is to be optimized subject to consumer acceptability constraints. This formulation directly reflects the stated goals of the competition.

Initial consumer acceptability constraints were obtained from current industry standards for midsized sedans (0-60mph acceleration<8sec and continuous gradeability>3.5%). Optimizations were performed on the six eligible architectures and the results are shown in Table 12. These vehicles represent the vehicles within each architecture with the highest E&EC Score that meet the consumer acceptability constraints.

Table 12 Optimized vehicle architectures

	Metric	Units	Constraint	S-H2 PFCV	P-E85 PHEV	P-B20 PHEV	P-E10 PHEV	S-E85 PHEV	S-B20 PHEV
Decision Variables	E&EC Score	--	Objective	0.838	0.797	0.767	0.722	0.688	0.638
	CD Range	mi	<80	79.99	79.99	80.00	79.97	79.94	79.49
	Acceleration	sec	<8	8.00	8.00	8.00	8.00	8.00	8.00
	Gradeability	%	>3.5	3.50	4.36	4.82	7.17	3.50	3.81
	Vehicle Mass	kg	--	1784	1786	1793	1827	1813	1818
Design Variables	Battery Energy	kWh	>5, <20	19.61	18.43	18.26	18.47	19.67	20.00
	Degree of Hybridization	--	>0.3, <0.9	0.67	0.67	0.65	0.58	0.69	0.67
	Vehicle Power	kW	>100, <180	121.27	134.89	139.81	157.93	123.13	124.69

Of the six architectures, plug-in fuel cell vehicles (PFCVs) obtain the best emissions and energy consumption scores followed by parallel E85 PHEVs and parallel B20 PHEVs. Series PHEVs perform slightly worse due to added componentry mass, added energy conversion steps, and subsequent energy losses. PFCVs have good scores due to their high operating efficiency, zero tailpipe emissions, low upstream carbon emissions, and minimal petroleum use. From Table 12, it can be seen that the upper battery energy constraint (or upper CD range constraint) is active for all architectures, which indicates

that increased electrification would further improve E&EC Score. Also, the acceleration constraint is active for all architectures indicating that E&EC Score could also improve if the acceleration constraint was relaxed. For the series PFCV and the series E85 PHEV the gradeability constraint is also active indicating E&EC score would improve if the gradeability constraint were relaxed. Interestingly however, the gradeability constraint is *not* active for other architectures suggesting the optimal solution exists within the constraints of the design space.

The epsilon constraint method was used on the six potential architectures to investigate the effect of increasing charge-depleting range while maintaining acceleration and gradeability constraints. The Pareto-optimal results are plotted Figure 23.

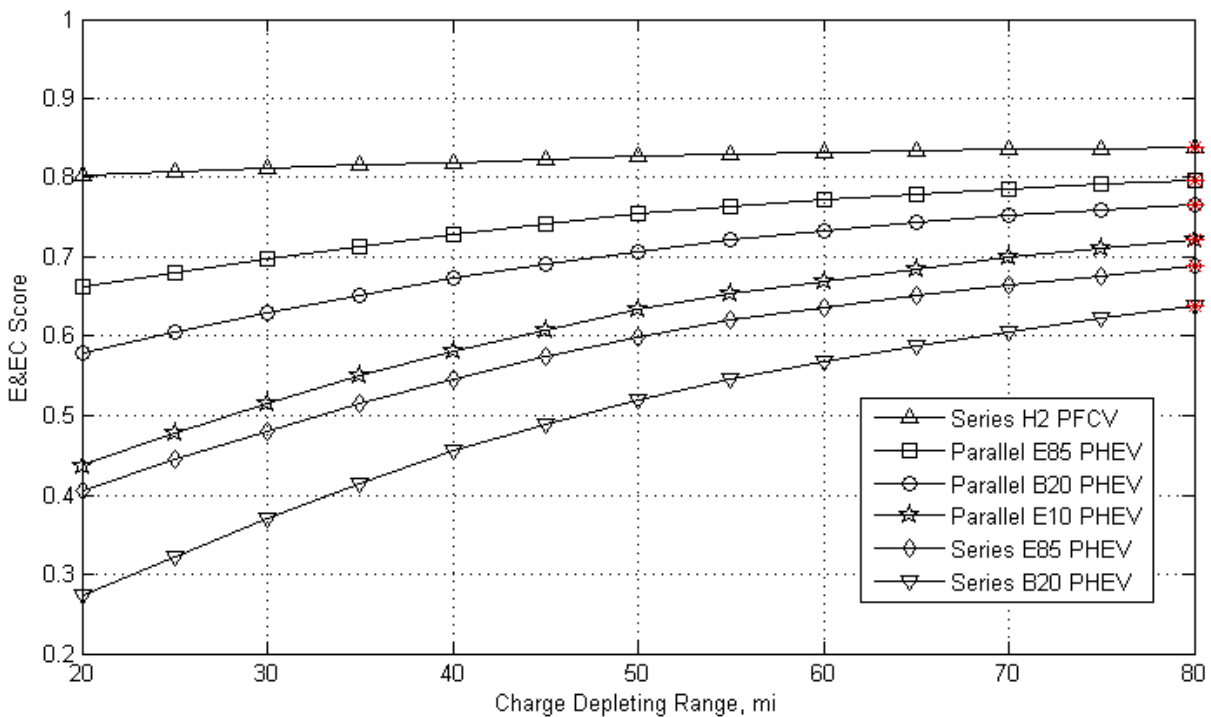


Figure 23 Pareto-optimal E&EC Score over CD range (subject to: 0-60mph<8sec and gradeability>3.5%)

As expected, all architectures benefit from increased charge-depleting range, but low scoring architectures display higher sensitivity to charge-depleting range than high scoring architectures. As the charge-depleting range increases, all designs converge towards electric vehicles, which is the highest E&EC scoring architecture.

Further analysis is provided in the next section, where competition-relevant tradeoffs are discussed and inverse design is performed. Tradeoffs include the effect of acceleration and gradeability constraints on E&EC score.

In this section, tradeoffs between the design objective and consumer acceptability constraints are quantified. From this analysis an informed decision on required acceleration time and gradeability can be made and the implications and compromises from that decision can be fully illuminated.

Utilizing the epsilon constraint method, a Pareto-optimal surface of E&EC score as a function of acceleration and gradeability was developed. A figure of the Pareto-optimal inverse design space was created where the x and y axes are design constraints and the design objective is plotted as a function of those constraints. The effect of the constraints on the vehicle's design variables was plotted adjacent to the E&EC plot. Finally the optimal solution from Table 12 is plotted in red within the design space. This analysis was performed for each vehicle architecture from the previous section. The results in the figures below represent an inverse design process where decision variables are controlled on a Pareto-optimal design space and design variables are communicated as results. To obtain an inverse design space, multiple optimizations were performed on the surrogate models.

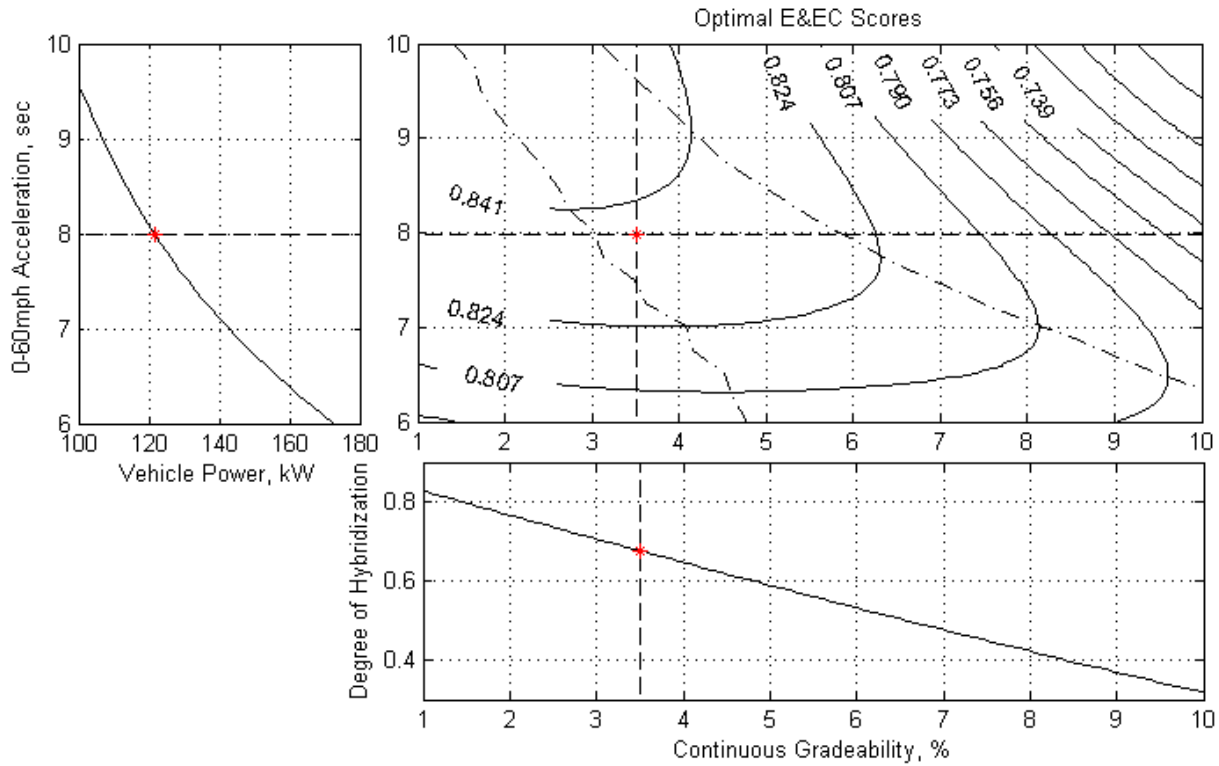


Figure 24 Series H2 PFCV Pareto-optimal inverse design space (optimized design point shown in red)

It can be seen in the figures above that, for any acceleration time, there exists a gradeability that maximizes E&EC score. The reverse is true as well; for any gradeability, there is an acceleration time that maximizes E&EC score. This can be thought of in terms of design variables too; for a given vehicle power, there exists a degree of hybridization that optimizes the E&EC score (and the reverse is true as well). Additionally, the results show that increasing severity of *both* acceleration *and* gradeability constraints leads to reduced E&EC scores. In terms of design variables; increasing the vehicle power *and* degree of hybridization leads to reduced E&EC score.

Within the gradeability-acceleration plane, shown in the figures above, there exists a Pareto-optimal design region. Outside this region, all designs are strictly dominated. The shape, size, and location of the Pareto-optimal design region differ for each architecture, but some trends are apparent. For parallel architectures the Pareto-optimal region is a narrow band within the acceleration-gradeability plane. This is likely due to the fact that, being coupled to the wheels, the average engine operating efficiency is

maximized at a specific engine power (on the specific drive cycles under the specific control strategy) which makes the optimal region quite narrow. For series architectures, the optimal design region is wider due to the advantage of the auxiliary power unit being decoupled from the driveshaft and therefore being able to operate at high efficiency under all driving conditions. Regardless of architecture or charge-depleting range, the non-dominated acceleration-gradeability region should be considered when selecting design constraints and resulting component sizes.

The tradeoff between the consumer acceptability constraints (acceleration and gradeability) and the goals of the competition (reduction of emissions and energy consumption) are clearly communicated in the figures above. Thinking of, and visualizing, the design space in terms of decision variables, as opposed to design variables, is a more intuitive and effective way to perform design decisions and communicate tradeoffs.

Based on this inverse design process, and further analysis of the team's resources and capabilities, the CSU design team chose to design and build a hydrogen fuel cell plug-in hybrid electric vehicle (PFCV). The team selected a high power 145kW electric motor from Unique Mobility (the optimal size, 125kW, electric motor could not be procured), an 18.9kWh, 177kW donated battery pack from A123, and a small, 12-15kW, fuel cell stack to minimize cost and weight, improve packaging, and minimize start-ups while maintaining range and performance. Rather than the conventional charge-depleting/charge-sustaining control strategy, the team is exploring a blended, charge-depleting mode strategy to take greater advantage of steady state, high efficiency operation of the fuel cell system and potentially increase the vehicle's performance and reduce the hydrogen storage requirement. Figure 25 is an illustration of the team's selected architecture, fuel choice and major component selections.

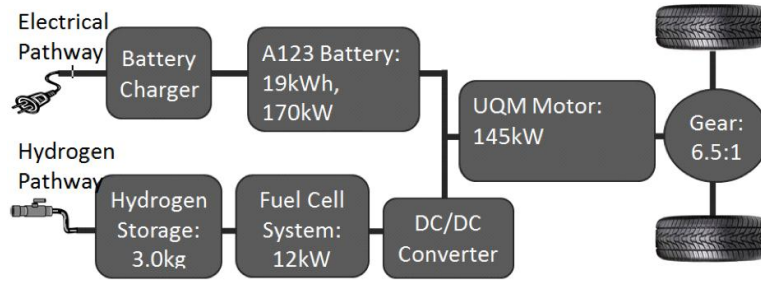


Figure 25 Selected Architecture, Fuel, and Components based on the results of this study

This research is an ongoing collaborative effort by the CSU design team. As component details are acquired, the vehicle models are updated and detailed design progresses. Some continued analyses include the determination of hydrogen storage requirements under various control strategies and driving scenarios, and optimization of the energy management control strategy of the vehicle.

The Decision Support System developed in this report utilized state of the art design tools including modeling and simulation of hybrid vehicle systems, and optimization of those systems in terms of decision relevant metrics to facilitate the use of inverse design. The approach that was taken, to develop surrogate models of the design space, enabled the design process to be reversed, where the decision maker had control over the decision variables as opposed to the design variables. This approach enabled effective communication of design tradeoffs that are inherent in multi-objective analysis and illuminated design space for decision makers. Based on the results of this research the team selected their fuel, architecture, and major components. The team is currently investigating ideas that further push the boundaries of conventional plug-in hybrid vehicle design philosophy by controlling the vehicle in a blended charge-depleting mode over the entire range to enable efficient fuel cell operation and possibly downsize the fuel cell even further.

Inverse design has the potential to improve advance vehicle design through elevating the decision maker's understanding of tradeoffs and thus improving design decisions and the resulting system design. Improved design will progress the state of the field and will lead to faster consumer acceptance of advanced vehicle technologies. Improved vehicle design processes, through inverse design, will positively affect the energy independence and environmental sustainability of the transportation sector.

5.0 Detailed Design and Control Strategy Development of a Plug-in Fuel Cell Hybrid Electric Vehicle for CSU's EcoCAR

Section 4.0 showed that PFCVs outperform all other EcoCAR2-admissible technologies based on EcoCAR2 metrics. Further, the study showed that a small fuel cell system and large battery create optimal performance. Based on this study, CSU's EcoCAR2 vehicle architecture was selected and major components were ordered. A full-functioning electric vehicle with a small onboard fuel cell system for extending the battery range was the highest performing architecture and was selected by the Colorado State University Team. The architecture block diagram is shown in Figure 25. It was decided that a large 19.8kWh, 177kW battery from A123 and a 145kW UQM electric motor were the closest to optimal size components that could be acquired. A small, 12kW, custom fuel cell stack was also proposed. The Architecture Selection Study prompted further questions: How small of a fuel cell stack can be built to still have a full functioning vehicle? What are the constraints on the fuel cell design? How should the fuel cell be controlled to produce optimal vehicle level performance? A custom fuel cell stack greatly expands the design freedom of the system but also increases the modeling and design complexity.

In the following sections we discuss a detailed design study of CSU's EcoCAR2 vehicle that utilizes the models and the decision support system created in the

Vehicle Modeling section. The versatility of the decision support system is demonstrated in the following sections.

5.1 Introduction

To answer the question of fuel cell sizing and supervisory control a more detailed and more representative fuel cell model was developed to replace the previous fuel cell in our vehicle model. The new fuel cell is representative of a highly passive system with a small balance of plant components, porous bipolar plates with parallel channels, and a wicking layer on the cathode side for improved water management [5]. The previous model was representative of a high power, highly controlled, automotive

fuel cell system with a large balance of plant (BOP) requirements. Figure 26 shows the fuel cell system efficiency curves that were developed from polarization curves and BOP requirements of each fuel cell model.

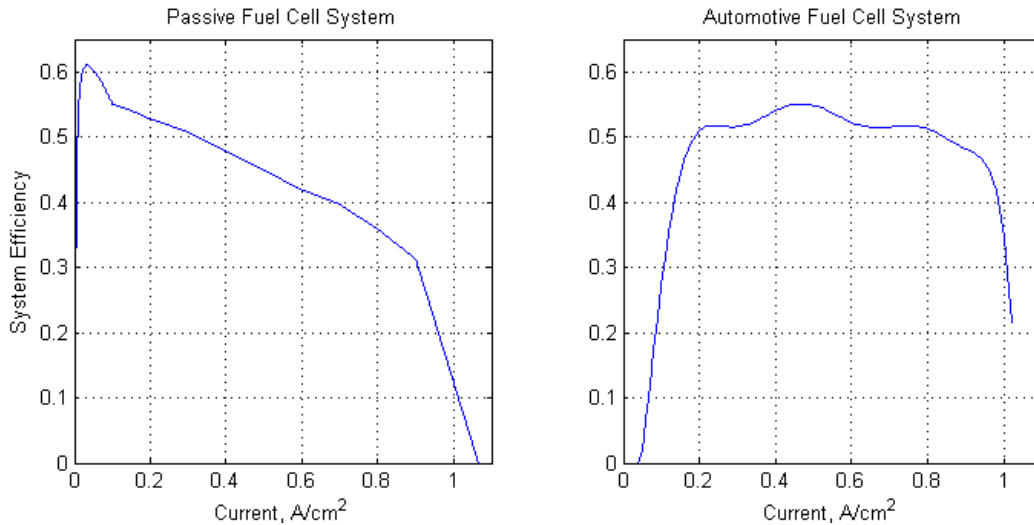


Figure 26 Passive fuel cell system efficiency (left), automotive fuel cell system efficiency (right)

After consulting the EcoCAR2 rulebook it was decided that the vehicle should be able to travel over 200 miles on the EcoCAR2 4-cycle test, but a charge-sustaining requirement was NOT necessary. This prompted the idea of having an electric mode and a blended charge-depleting mode control strategy to meet the 200mile range requirement. The electric mode would provide a small amount of range with the fuel cell off, thus gaining the benefits of utility factor. The blended mode would provide additional vehicle range while still depleting the battery. This control strategy is represented in Figure 27.

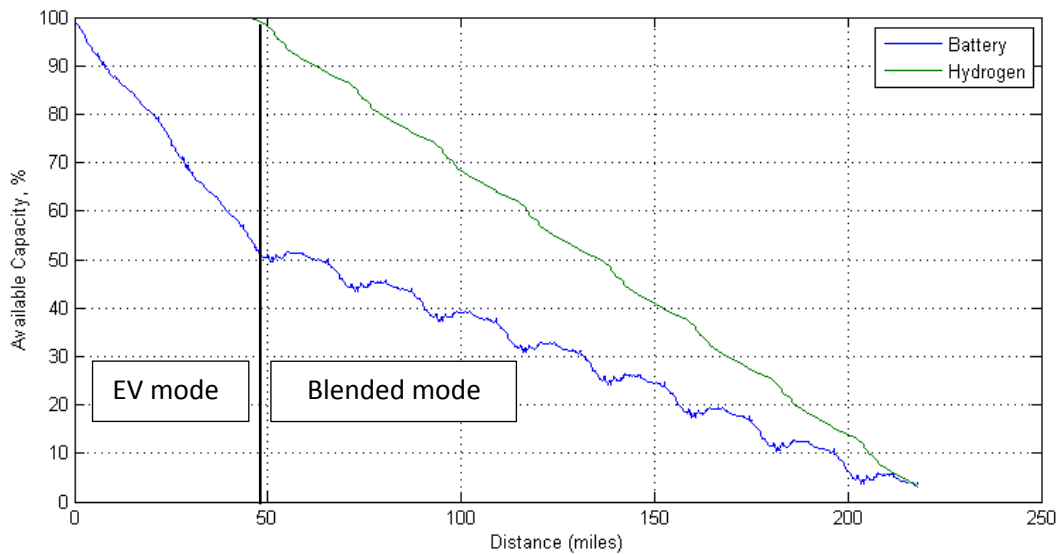


Figure 27 Electric only to blended-charge-depleting control strategy representation

To gain the 200mile range requirement, the fuel cell would need to be turned on earlier in the driving. Because all EcoCAR2 evaluation metrics are based on utility-factor-weighting, increased utility factor is beneficial in the competition. But clearly utility factor will come at the cost of operating the fuel cell at higher power and lower efficiency. How does this tradeoff translate to the overall vehicle performance as far as the competition is concerned? Also, as it is a custom fuel cell stack, what is the optimal stack size? Lastly, how much onboard hydrogen should be stored to reach or exceed the 200mile range requirement? Previously it was proposed that 3.6kg would be required, but with the new fuel cell model is this still true?

The following study documents the process by which the CSU team has tackled these design questions. The results are presented and design decisions are made.

5.2 Methods

The updated model's subsystems utilize vendor-supplied performance data of each component that will be acquired. In this way the model is as representative of the physical system as possible at this time. The design variables in this case include fuel cell peak power and fuel cell operating power. The

vehicle is simulated in EV mode and Blended mode on the EcoCAR2 4-cycle test. Results are post processed to calculate competition metrics such as UF-weighted total energy consumption (Wh/km), UF-weighted WTW petroleum energy use (Wh/km), UF-weighted WTW GHG emissions (g/km), and UF-weighted WTW criteria emissions (bins). Finally each metric is normalized against a database of previously simulated designs from section 4.0 and the total EcoCAR2 score is calculated.

5.3 Results

A design of experiments was performed to determine the optimal fuel cell size and control strategy. In this section the results from the DOEs are presented. Some key results are highlighted and a Pareto-optimal tradeoff is identified which is discussed in the concluding section.

5.3.1 EV Range vs Competition Score

Figure 28 shows the vehicle's EV range over the design space. This plot allows us to identify the constraints on the design space. Vehicles with zero EV range are operated all the time in blended mode and may not be capable of reaching the 200mile requirement. It can be seen that, with the selected components, a fuel cell operating power of about 6kW is sufficient to reach the 200mile range requirement, but below 6kW the vehicle may be unable to meet the required range. It can also be seen that operating powers greater than 18kW enable the vehicle to be charge-sustaining and utilize all the battery in EV mode thereby maximizing the utility factor.

From Figure 29 it can be seen that the efficiency benefits of low power fuel cell operation outweigh the cost of lost utility factor. The optimal design exists along the boundary where the vehicle is a purely blended charge depleting vehicle with no electric-only range, Figure 30. The fuel cell should be operated at low power over the entire driving range to maximize EcoCAR2 score.

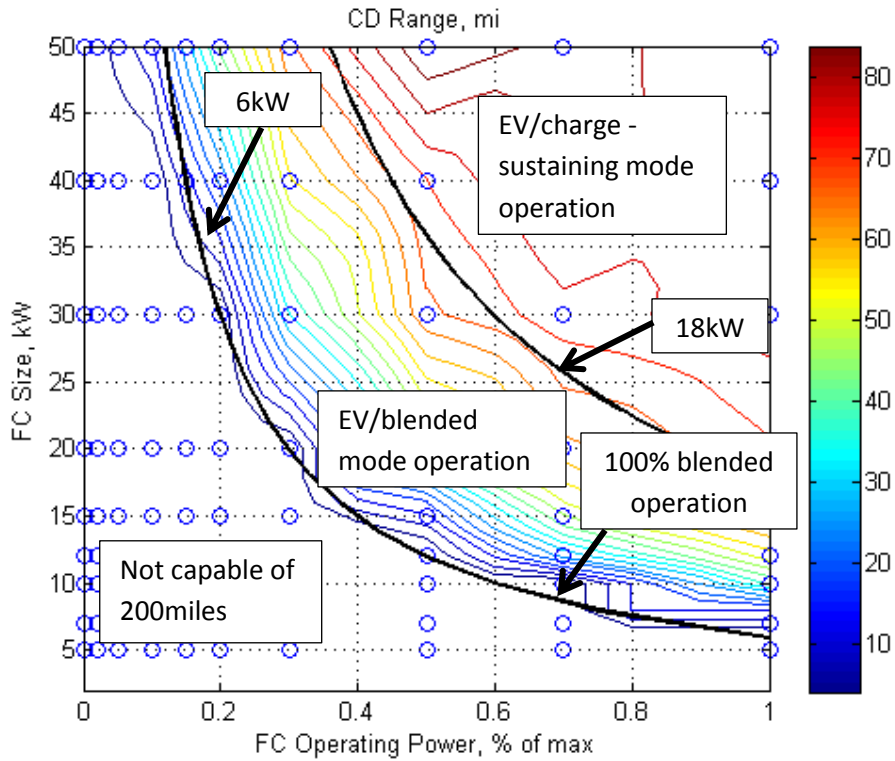


Figure 28 EV Range vs FC power and operating point

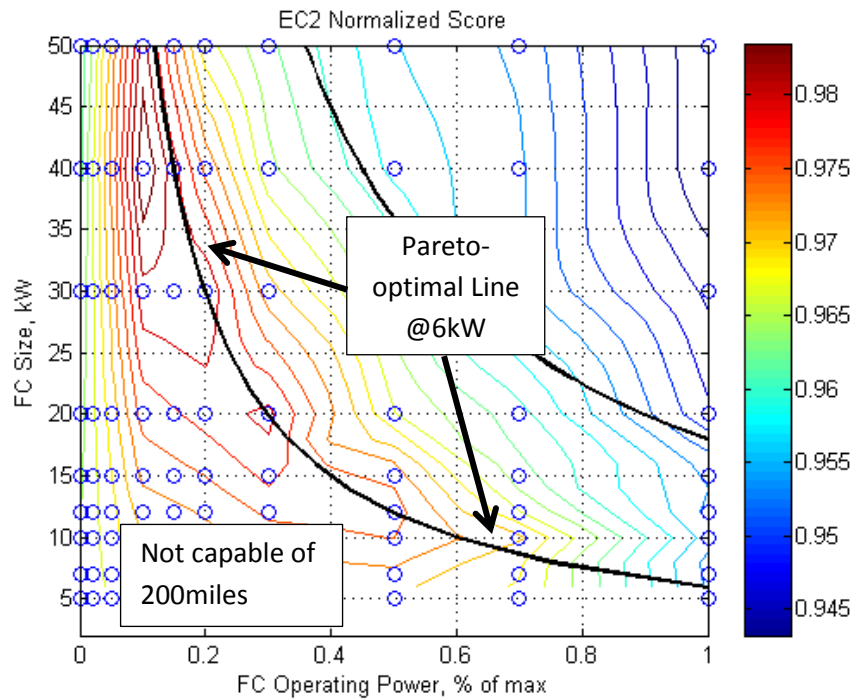


Figure 29 EcoCAR2 Score vs Fuel Cell size and operating point

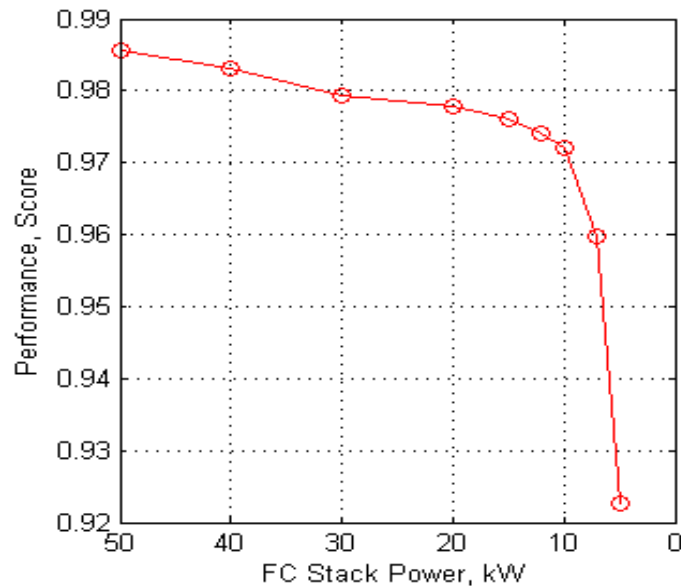


Figure 30 Pareto tradeoff between EcoCAR score and fuel cell system power using the optimal blended charge depleting control strategy

5.3.2 Supervisory Control Strategy Development

With the knowledge that a blended mode strategy is optimal, the challenge is to design a supervisory control strategy that maximizes range and EcoCAR2 score while maintaining full vehicle functionality throughout the driving range under variable driving conditions. Essentially we want the fuel cell to operate at a steady power output such that both the hydrogen tanks and the battery reach zero state-of-charge simultaneously. A PI controller with low gains to minimize the state-of-charge difference between the hydrogen tank and the battery will produce a flexible control strategy that meets our goals. A block diagram of the control strategy is shown in Figure 31 and an illustration of the control strategy in action is shown in Figure 32 and Figure 33. Figure 34 shows how the supervisory control system works when the energy consumption changes drastically. Next, the controller gains must be tuned to produce the highest driving range possible and therefore the lowest energy consumption. The control gain tuning was performed and it was clear that a Proportional (P) gain of 3.5 and an Integral (I) gain of 0.0025 will produce the highest drivetrain efficiency and therefore the longest range for the EcoCAR2 drive cycles.

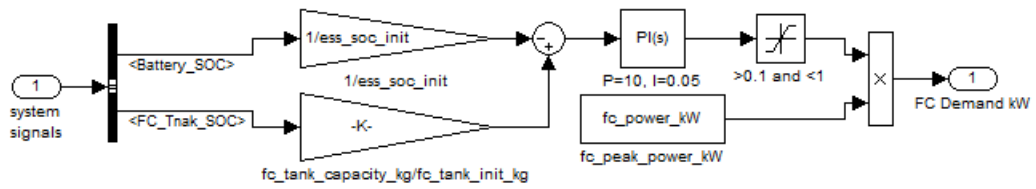


Figure 31 Supervisory control strategy diagram

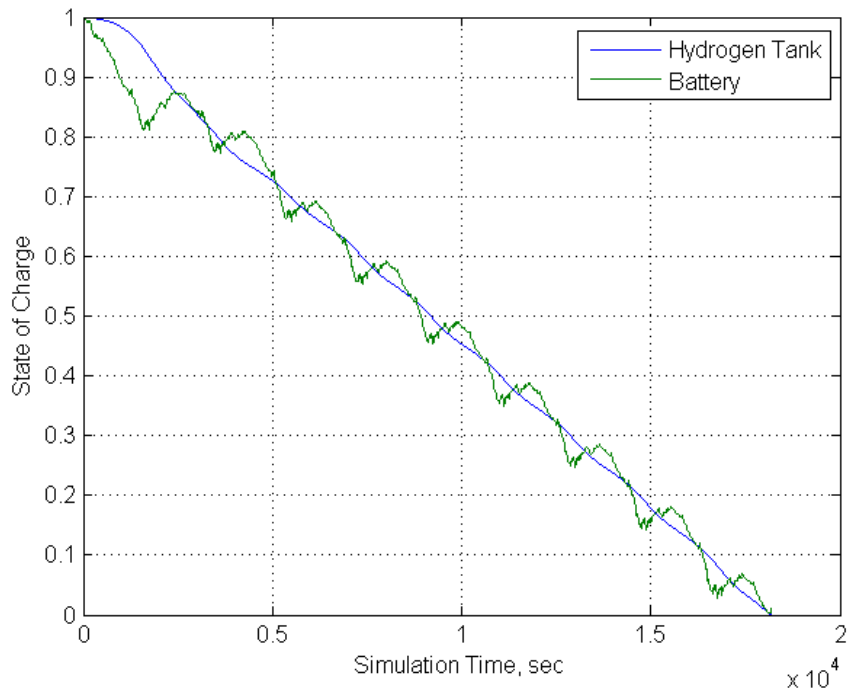


Figure 32 State of charge of battery and hydrogen tank under the blended charge depleting control strategy

Figure 32 shows the state of charge of both the battery and the fuel tank over repeated EcoCAR drive cycles. It is clear that the battery takes the transient load while the fuel cell operates at a steady state. The battery and the fuel tank are fully depleted simultaneously thus maximizing the vehicles fully functional range.

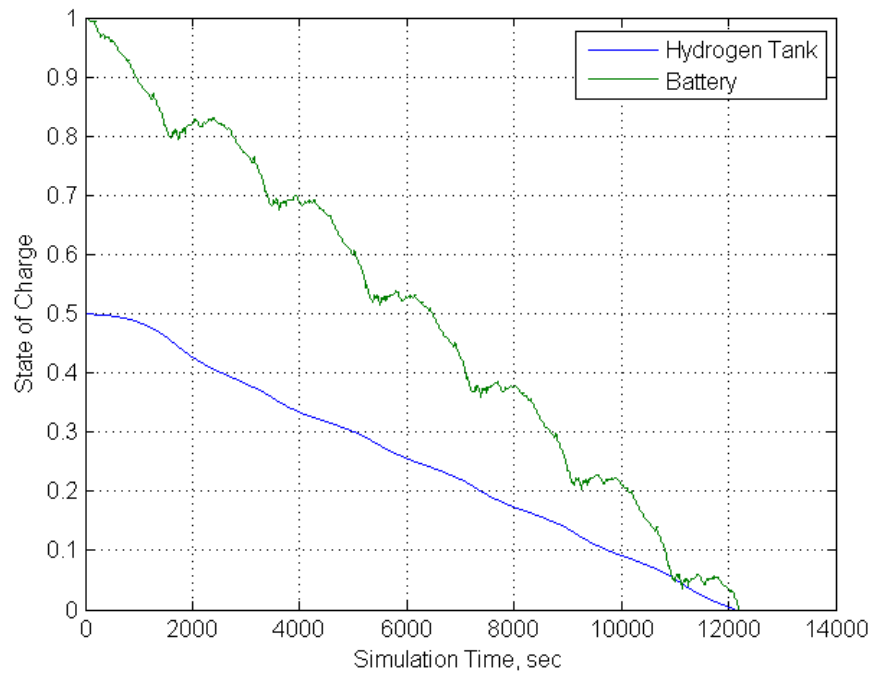


Figure 33 State of charge of battery and tank (with tank starting at 50%)

Figure 33 shows that the control strategy works for various initial states of charge for both the fuel tank and the battery. The fuel cell demand is adjusted based on initial tank capacities (at the start of the drive).

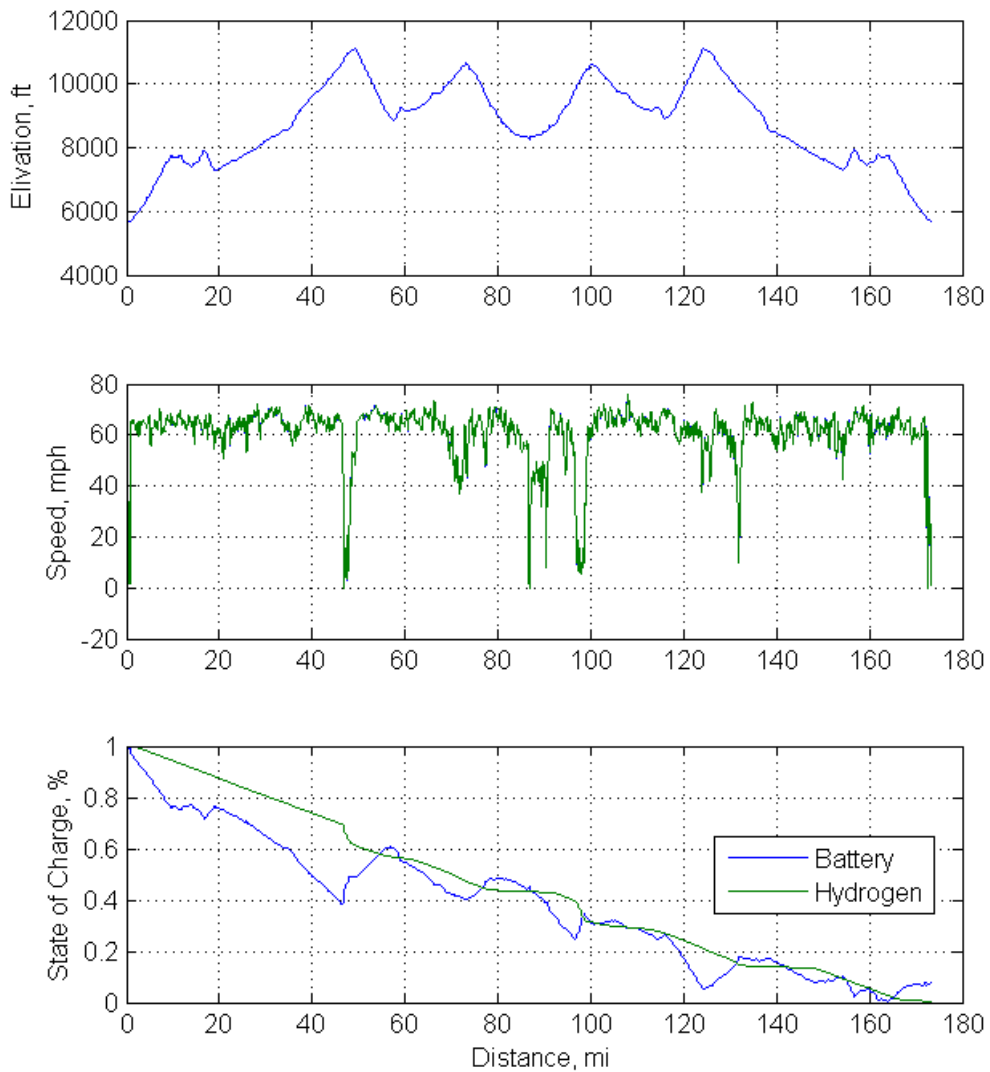


Figure 34 Control strategy in variable driving conditions (NREL to Vail, CO and back)

In Figure 34 we see the control strategy on variable drive conditions. The vehicle is able to achieve a simulated trip from Denver to Vail and back to Denver without seeing reduced performance at any point. This is impressive considering the fuel cell power is only 15kW and the battery is roughly 20kWh.

5.4 Discussion

With the supervisory control strategy designed, the Pareto-optimal tradeoff was identified as the boundary at which the vehicle is a purely blended mode charge-depleting vehicle that achieves 200 miles. The Pareto-optimal tradeoff exists between vehicle energy consumption (or competition score), hydrogen storage requirement, and fuel cell stack size. It can also be thought of as a cost vs. benefit tradeoff, as fuel cell power comes at a cost and the benefit is clearly energy consumption and saved hydrogen storage.

The cost vs. benefit analysis is shown below. For the CSU EcoCAR2 Team the stack size of the vehicle will be dependent on the progress achieved by the fuel cell development team. Ideally the team will have the capability to develop a 20-30kW stack but a 12-15kW stack is also acceptable and will perform well in the competition. Depending on the fuel cell stack size, between 2.5 and 3kg of hydrogen will be required to meet the 200mile range requirement. Another variable that is still uncertain is the tire rolling resistance. The team is hoping to acquire tires with C_{rr} as low as 0.0065 but the stock Malibu tires are about 0.008. The figures below show results with both tire models to illustrate the sensitivity to this variable.

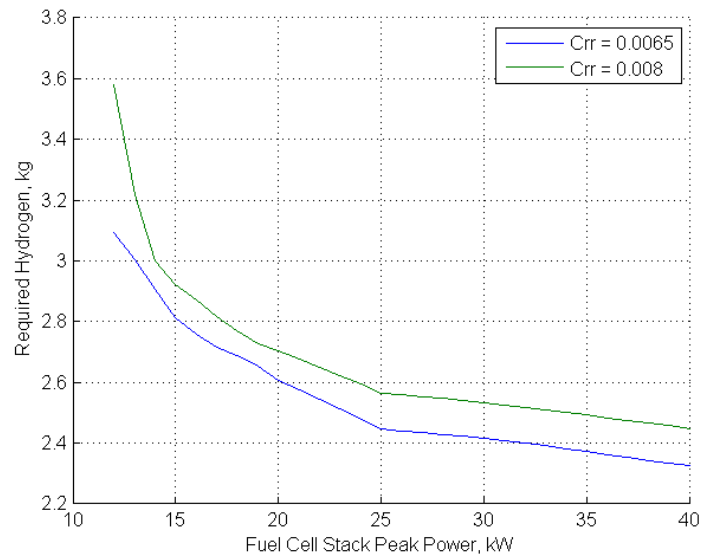


Figure 35 Required hydrogen for 200 miles as a function of fuel cell stack power

6.0 Conclusions

This thesis has pointed out findings and contributions to the field of advanced vehicle design and argued that improved technology assessment and high level design can be achieved through a broader look at technologies and development of flexible and interactive decision support systems.

First I presented vehicle models that were developed in MatLab/Simulink and have the advantage of being parameterized, customizable and able to be run efficiently and iteratively. This has the advantage over Autonomie, the current state of the field, in that customization and optimization can be performed at lower computational cost and, and with more control over the vehicle function.

Next, I presented a case study in which the vehicle models were used to perform a technology evaluation of plug-in fuel cell vehicles. In this study, we looked at a range of component sizing to understand the capability of each technology. The advantage in this approach lies in the fact that technologies can be viewed more as a set of data rather than a single data point. This approach has the advantage of tying vehicle simulation and component sizing optimization to decision metrics, and letting the decision maker decide how to formulate the cost function. This approach allows some insight into the tradeoffs within each technology and across technologies.

Next, a case in which a decision support system was used to perform powertrain optimization and technology assessment for the EcoCAR2 competition was presented. Vehicle models were connected to a system level decision variable, EcoCAR2 competition score, and were optimized. It was shown that, if properly implemented, a plug-in fuel cell hybrid electric vehicle will mathematically dominate the other alternatives in the EcoCAR2 competition.

Finally, the models and the decision support system were used to perform detailed design and evaluate Pareto-optimal tradeoffs for the selected EcoCAR2 vehicle. A control strategy was proposed that maximizes efficiency and range while minimizing the required hydrogen storage and the fuel cell stack size.

7.0 References

- [1] Kordesch, K. "The Kordesch Fuel Cell-Battery Hybrid Passenger Car", pp. 257-265 in Fuel Cells and their Applications by K. Kordesch, VCH Verlagsgesellschaft, Weinheim, Germany 1996.
- [2] Kalhammer F. "Hybridization of Fuel Cell Systems," in Plug-in Hybrid Electric Vehicle Workshop at 20th International Electric Vehicle Symposium, 15 November 2003, Long Beach, California.
- [3] Suppes, G.J., Lopes, S., and Chiu, C.W. "Plug-in Fuel Cell Hybrids as Transition Technology to Hydrogen Infrastructure." International Journal of Hydrogen Energy 2004; 29: 369-74.
- [4] Plug-in Fuel Cell Vehicle Technology and Value Analysis Phase 1: Preliminary Findings and Plan for Detailed Study. EPRI, Palo Alto, CA: 2010. 1021482.
- [5] Fabian, T., Hayre, O.B., Lister, S., Prinz, F.B., and Santiago, J.G., "Passive Water Management at the Cathode of a Planar Air-breathing Proton Exchange Membrane Fuel Cell." Journal of Power Sources 195 (2010) 3201-3206.
- [6] Society of Automotive Engineers. Utility Factor Definitions for Plug-In Hybrid Electric Vehicles Using 2001 U.S. DOT National Household Travel Survey Data. Hybrid Committee, March 2009; J2841.
- [7] Society of Automotive Engineers. Recommended Practice for Measuring the Exhaust Emissions and Fuel Economy of Hybrid-Electric Vehicles. Hybrid Committee, March 1999; J1711.
- [8] U.S. Environmental Protection Agency, "Fuel Economy Labeling of Motor Vehicle Revisions to Improve Calculation of Fuel Economy Estimates" EPA420-R-06-017, December 2006, available at: <http://www.epa.gov/fueleconomy/420r06017.pdf>.
- [9] U.S. Energy Information Administration, "Energy Prices by Sector and Source." Annual Energy Outlook 2012 Early Release. Available at: <http://www.eia.gov/forecasts/aeo/er/>
- [10] Joseck, F., "Systems Analysis." 2011 Annual Merit Review and Peer Evaluation Meeting, U.S. Department of Energy, May 2011, available at: http://www.hydrogen.energy.gov/pdfs/review11/h2pn04_joseck_an_2011_o.pdf

- [11] Argonne National Laboratory, The greenhouse gases, regulated emissions, and energy use in transportation (GREET) 1.8d model. Argonne, IL; 2010.
- [12] EcoCAR2, Plugging into the Future: <http://www.ecocar2.org/about-ecocar2>. .
- [13] Bradley, T.H. and Frank, A.A., “Design, demonstration and sustainability impact assessments for plug-in hybrid electric vehicles,” *Renewable & Sustainable Energy Reviews*, doi:10.1016/j.rser.2007.05.003, 2007.
- [14] Messac, A., “From Dubious Construction of Objective Functions to the Application of Physical Programming,” *AIAA Journal*, Vol. 38, No. 1, January 2000, pp.155-163.
- [15] Gao, W. and Porandla, S.K., “Design Optimization of a Parallel Hybrid Electric Powertrain,” IEEE, Center for Advanced Vehicular Systems, Mississippi State University, MS, USA, 2005.
- [16] K. Wipke, and T. Markel, “Optimization techniques for hybrid electric vehicle analysis using ADVISOR,” *Proc. ASME*, International Mechanical Engineering Congress and Exposition, New York
- [17] PSAT Documentation: <http://www.transporation.anl.gov/software/PSAT>.
- [18] Autonomie Documentation: <http://www.autonomie.net/>.
- [19] MatLab Neural Network Fitting Documentation:
<http://www.mathworks.com/help/toolbox/nnet/ref/nftool.html>.
- [20] Fox, M., Geller, B., Bradley, T. H., “A Simulation Integrated Decision Support System for Advanced Vehicle Design Demonstrated on Colorado State’s EcoCAR,” IECEC/JPC, August, 2012
- [21] Fox, M., et. al., “Plug-in Fuel Cell Vehicle Technology and Value Analysis,” 26th Electric Vehicle Symposium , Los Angeles, CA, May 2012
- [22] Simpson, A., “Full-Cycle Assessment of Alternative Fuels for Light Duty Vehicles in Australia,” Sustainable Energy Research Group, School of Information Technology and Electrical Engineering, The University of Queensland, Australia